ФИЗИКА ЭЛЕМЕНТАРНЫХ ЧАСТИЦ И АТОМНОГО ЯДРА
2004. Т. 35. ВЫП. 6

УДК 539.125.5

SPIN ASSIGNMENT OF NEUTRON RESONANCES VIA (n, γ) AND (n, α) REACTIONS

F. Corvi

EC-JRC, Institute for Reference Materials and Measurements, Geel, Belgium

M. Przytula

The College of Computer Science, University of Lodz, Poland

ФИЗИКА ЭЛЕМЕНТАРНЫХ ЧАСТИЦ И АТОМНОГО ЯДРА
2004. Т. 35. ВЫП. 6

УДК 539.125.5

SPIN ASSIGNMENT OF NEUTRON RESONANCES VIA (n,γ) AND (n,α) REACTIONS

F. Corvi

EC-JRC, Institute for Reference Materials and Measurements, Geel, Belgium

M. Przytula

The College of Computer Science, University of Lodz, Poland

Several methods exist, and have been used in the past, for determining the spins of neutron resonances. However the present review is limited to those techniques which exploit the spin dependence of (n,γ) and (n,α) spectra. These methods, which turned out to be very productive, are essentially based on the systematics of the γ and α decay for the various multipolarities. In the case of radiative capture, two methods, and the results achieved, are described in detail: *i) the multiplicity method; ii) the low-lying level population method*. Both techniques apply to those compound nuclei for which radiative capture can be described by the statistical model, namely most nuclei with atomic weight $A > 90-100$, with the possible exception of those having magic or near-magic proton or neutron numbers. The first method has the merit of having provided large amounts of spin assignments at times which were technologically less advanced than the present ones: its main drawback however is the fact of not being applicable to odd–even target nuclei. The second method is not subject to this limitation while presenting at the same time spin effects much larger than those of the multiplicity method. The obtained results have been used to provide estimates of the spin cut-off parameter σ and to study the possible spin dependence of the s-wave neutron strength function. Spin assignments of p-wave resonances have helped in the analysis of the parity nonconservation measurements performed by the TRIPLE thus improving the estimates of the weak spreading width Γ_w. In this context it has been found that the population of the low-lying states depends significantly not only on the parity of the initial state. Finally, spin assignments based on (n,α) reaction are described for the target nuclei ^{143}Nd and ^{147}Sm.

Существует несколько методов, которые уже использовались ранее, для определения спинов нейтронных резонансов. Однако в настоящем обзоре мы ограничились теми, которые используют спиновую зависимость (n,γ)- и (n,α)-спектров. Эти методы, весьма продуктивные, естественно базируются на систематиках γ- и α-распадов для различных мультипольностей. В случае радиационного захвата детально описываются два метода, основанные а) на измерении множественности и б) на определении заселенности низколежащих уровней, а также полученные результаты. Обе методики опираются на возможность использования статистической модели, т. е. для ядер с атомным весом $A > 90-100$, с возможным исключением ядер, имеющих магические или околомагические числа протонов или нейтронов. Первый метод имеет то преимущество, что с его помощью получена спиновая идентификация большого количества нейтронных резонансов, его основной недостаток состоит в том, что он неприменим для нечетно-четных ядер-мишеней. Второй метод не обладает таким ограничением, поскольку здесь спиновый эффект больше, чем для метода множественности. Результаты анализа использовались для получения параметра спинового обрезания σ, а также для изучения возможной спиновой зависимости силовой функции для s-волновых нейтронов. Определение спинов для p-волновых резонансов помогло при анализе измерений нарушений пространственной четности, проводимых коллаборацией TRIPLE,

что позволило улучшить оценку «спредовой» ширины слабого взаимодействия Γ_w. При этом было обнаружено, что заселение низколежащих состояний существенно зависит не только от спина, но и от четности начального состояния. В конце описывается определение спинов для ядер-мишеней ^{143}Nd и ^{147}Sm с помощью реакции (n, α).

INTRODUCTION

The knowledge of the spins of neutron resonances is important on many grounds. First of all, it allows one, in combination with total and partial cross-section measurements, to determine unambiguously the partial widths of any given resonance by fixing the value of the spin statistical factor g present in the Breit–Wigner formula. Secondly, the determination of the spin of large samples of resonances is needed in order to study the (possible) spin dependence of quantities such as the neutron strength function, the total radiative capture width and, when applicable, the average fission width. Similarly, this kind of data allows a check of the spin-dependent part of the level density formula based on the statistical model. In this context it is particularly interesting to determine the value of the spin cut-off parameter σ which has been the object of many studies. Moreover, if a complete sample of resonances of the same spin and parity can be selected in a given energy interval, this gives the opportunity to check the Orthogonal Ensemble statistics of Dyson and Mehta [1], which foresees long range correlations of the energy eigenvalues of nuclear levels. Finally spin values of s- and particularly p-wave resonances are necessary for the interpretation of parity violation studies of compound nuclear states as it will be shown in Sec. 2.

Several methods exist, and have been used in the past, for determining the spin of neutron resonances. However the present review is limited to those techniques which exploit the spin dependence of (n, γ) and (n, α) spectra. These methods, which turned out to be very productive, are essentially based on the systematics of the photon strength functions for various multipolarities: see, for example, Ref. 2 for a discussion of these quantities, including their energy and atomic mass dependence, and their comparison with compilations of experimental values derived from both neutron capture and photonuclear experiments. To summarize in a very rough way, it can be stated that for medium weight and heavy nuclei, and for energies of the order of the neutron separation energy, the partial radiation widths of dipole transitions are on average much larger than those of quadrupole ones. Moreover the widths of the electric $E1$ and $E2$ transitions are typically an order of magnitude larger than those of the corresponding $M1$, respectively, $M2$ magnetic transitions.

It should be pointed out however that these rules hold in general for the so-called continuum part of the excited level scheme of the compound nucleus but not for the discrete part at lower excitation energy where, for example, $E2$ transitions play a dominant role in the case of even–even nuclei.

From what just said it would appear that the most straightforward way of assigning the resonance spins would be to measure the intensities of those primary gamma rays ending at low-lying levels of known spin and parity. Although quite a few resonance spins have been determined in this way [3, 4], we don't consider this a general method of spin assignment for at least two reasons: firstly, the Porter–Thomas fluctuations of the intensities of primary gammas tend to blur the effect so that it is not always safe to assign the multipolarity of a transition on the basis of its strength. Secondly, observation of these high energy γ rays is hindered by the very low photopeak efficiency of the Ge detectors used: since in many cases the observability thresholds are comparable with the expected widths of the $E1$ transitions, the fact of not observing a given gamma peak does not provide any information on the initial spin.

The measurement of the intensities of two-step cascades to the ground or to some low-energy state largely removes such fluctuations and still exhibits an important spin-dependent effect [5]. However, the method can only be applied when it is possible to isolate transitions to one or few final states with high efficiency gamma-ray detectors. The methods discussed in this review are not only substantially free from the effect of Porter–Thomas fluctuations, since the measured quantities are the cumulative result of hundreds or thousands of different gamma cascades, but they are also of large efficiency. This allows one to determine the spins of most, if not all, of the resonances observed in the investigated energy range. These methods are:

i) *the multiplicity method*;

ii) *the low-lying level population method*.

The first one, and the results achieved, will be described in Sec. 1. Application of the second method to both s-wave and p-wave resonances will be treated in Sec. 2. It will be shown that the low-level population method can also be applied to the determination of the resonance parity. In Sec. 3 the obtained results will be used to investigate the spin dependence of nuclear quantities such as the level density and the neutron strength function. Finally, the spin assignment of neutron resonances via the (n, α) reaction will be dealt with in Sec. 4.

It should be stressed that the application of the methods just described is restricted to medium-weight and heavy compound nuclei with high-level density in which radiative capture in the continuum zone can be described with the statistical model.

1. THE MULTIPLICITY METHOD

This method was successfully proposed in the late sixties by Coceva et al. [6, 7]: a considerable body of data was collected at the electron linac of Institute

for Reference Material and Measurements (former CBNM), Geel, Belgium. Later on the method was extensively used in Dubna with different detector types.

1.1. Principle of the Method. In the following one deals only with neutron resonances having zero angular momentum ($l = 0$) so that only two spin states are possible: $J = I - 1/2$ and $J = I + 1/2$, where I is the spin of the target nucleus. Assuming that radiative capture mainly proceeds via dipole transitions, the spin change involved at each step of a given gamma cascade is mostly zero or one. It seems then reasonable to assume that the average number of steps per cascade is influenced by the spin difference between the initial and the final state. Some experimental indication for this effect was obtained by Draper and Springer in their measurements of average multiplicity [8]. In a more general approach, we may say that the spin of the excited state formed in neutron capture should affect both the average value and the distribution of the multiplicity, i.e., of the number of emitted gammas per capture. Consequently also the gross structure of the γ-energy spectrum should be spin-dependent.

From the experimental point of view, a quantity related to the multiplicity can be most easily measured with an apparatus composed of two or more γ detectors of which both the single S_i and the coincidence C_i rate are recorded for any given resonance i with spin J. A simple expression for the ratio $R_J = S_i/C_i$ can be derived by making some simplifying assumptions. Let us suppose that each detector subtends the same solid angle Ω with respect to the sample and that Ω be small as compared to unity. Neglecting then angular correlations of γ rays and assuming that the γ detectors have unit intrinsic efficiency for γ rays of any energy, one gets the simplified expression:

$$R_J = 2\langle\nu_J^S\rangle/[\langle\nu_J^C(\nu_J^C - 1)\rangle\,\Omega(n-1)], \tag{1}$$

where n is the number of detectors, the brackets indicate an average over all cascades, and ν_J^S and ν_J^C are the respective multiplicities as seen by the two detection systems, i.e., the number of γ rays per cascade with the energy higher than the chosen lower thresholds E_T^S and E_T^C corresponding to single and coincidence counts, respectively.

To ensure a relatively high coincidence efficiency, the coincidence threshold is kept as low as possible so that $\nu_J^C \cong \nu_J$. The singles threshold E_T^S is then varied so as to increase the relative difference between the two values of R_J corresponding to the two spins of the initial states. For the nuclei studied, it was found empirically that such a difference increases noticeably with E_T^S; this behaviour can be intuitively understood by considering that an increase in multiplicity gives rise to a softer gamma spectrum.

In order to verify in a more quantitative way the qualitative considerations developed so far, a numerical simulation of the radiative capture process based on the Monte Carlo method was performed for a few even–even compound

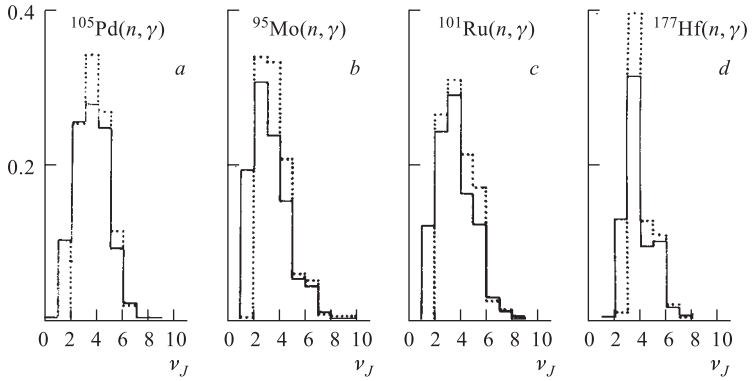

Fig. 1. Calculated frequency distributions of the gamma-cascade multiplicity for the two spin values of s-wave resonances in target nuclei ^{105}Pd (a), ^{95}Mo (b), ^{101}Ru (c), ^{177}Hf (d). Solid line — $J = 2$ (a, b, c), $J = 3$ (d); dotted line — $J = 3$ (a, b, c), $J = 4$ (d)

nuclei. Weisskopf and Moszkowski formulae were summed for the dependence of electric and magnetic multipole transition probabilities on the energy of the emitted gamma. The actual spectrum of excited levels was introduced up to an excitation energy below which energy, spin, parity and branching ratios for gamma decay were experimentally known for every level considered. Above such an energy, a continuum of levels was assumed, governed by the level density formula derived from Bethe's free gas model [9]. More details on the program can be found in Refs. 7, 10.

The output of the code provides estimates of the distribution of the multiplicity ν_J, of the total and primary γ-energy spectra, and of the numerator and denominator of expression (1). In Fig. 1 the calculated multiplicity distributions are plotted for the two spin values of s-wave capture in the target nuclei ^{105}Pd, ^{95}Mo, ^{101}Ru, and ^{177}Hf: one may note that in all four cases the distribution for the spin $J = I + 1/2$ is shifted towards higher values with respect to the corresponding one for $J = I - 1/2$.

The difference is not large but it is further magnified in the denominator of Eq. (1), where the square power of ν_J appears. The behaviour of the singles multiplicity ν_J^S is described in Fig. 2 where the ratio $\langle \nu_3^S \rangle / \langle \nu_4^S \rangle$ is plotted versus the singles threshold E_T^S for the reaction ^{177}Hf(n,γ): one may notice that the ratio increases with the threshold becoming larger than unity above 2 MeV.

Therefore if the threshold is set above this value, the singles yield is lower for the spin state with higher multiplicity, a fact which confirms our experimental finding. It follows that the numerator and the denominator of Eq. (1) are a decreasing and, respectively, an increasing function of ν_J making the ratio R_J

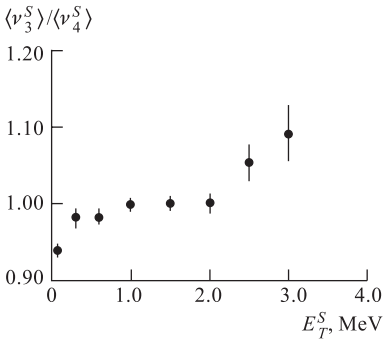

Fig. 2. Calculated ratio of the average number of gamma rays above threshold per neutron in ^{177}Hf resonances with spin $J = 3$ and, respectively, $J = 4$ as a function of threshold energy E_T^S

more sensitive to the spin effect. It seems then reasonable to work with a very low threshold for coincidence and a high threshold for single counts; this choice is also the most suitable to keep a fairly high count rate for coincidences and to optimize the signal-to-background rate for singles. The singles threshold cannot be set too high lest the Porter–Thomas fluctuations of the limited number of accepted transitions can blur the J-dependent effect.

Finally, we define as a figure of merit d for the effect or «spin effect index» the relative difference between the two values of R_J corresponding to the two spin values:

$$d = 2(R_{I-1/2} - R_{I+1/2})/(R_{I-1/2} + R_{I+1/2}).$$

In Fig. 3 are plotted, as a function of the singles threshold, the calculated values of d with their errors as estimated from the finite statistics. These errors are possibly overestimated because the two simulations corresponding to the two spin states are correlated by the use of the same sequence of random numbers. The experimental values, represented by full triangles, compare well with the calculated ones except in the case of ^{105}Pd where they are definitely higher. One may finally observe that in the case of ^{177}Hf with $I = 7/2$ the effect is considerably less than in the other isotopes with $I = 5/2$: this finding is quite understandable if one considers that the relative difference in multiplicity tends to decrease by increasing the difference between initial and final spin value.

At JINR, Dubna, von Egidy's code of capture gamma-ray simulation [11] was applied to this specific problem and results consistent with those just mentioned were obtained [12, 13]: an example is given in Table 1 where there are listed the γ-ray multiplicities calculated as a function of the energy of the lower threshold for the two spin states of the reaction ^{147}Sm(n, γ). One may notice that the effective multiplicity for the $J = 4$ state, which is higher than that of the $J = 3$ state at low thresholds, becomes lower at thresholds larger or equal to 1.5 MeV. This result is in agreement with the plot of Fig. 2.

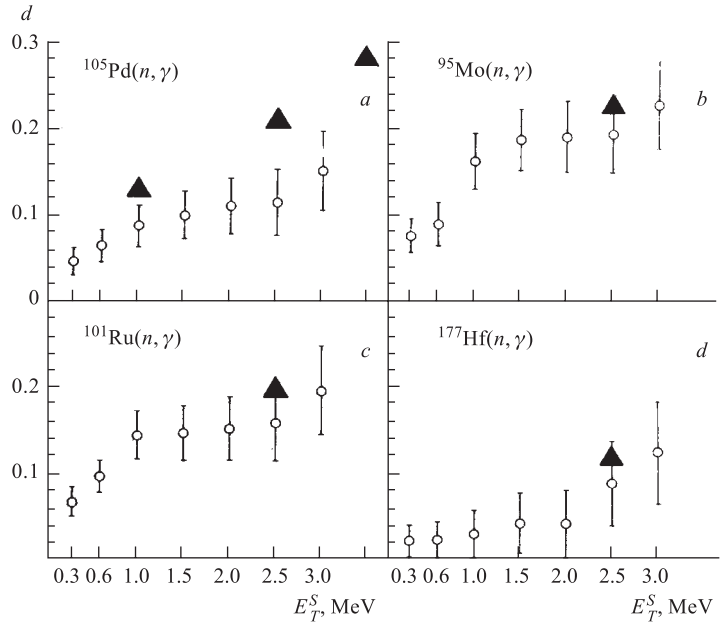

Fig. 3. Calculated (open circles) and experimental (full triangles) values of the spin effect index d as a function of the energy threshold for single counts E_T^S for the target nuclei of Fig. 1

Table 1. **Calculated effective multiplicity for ^{147}Sm(n,γ) for different thresholds and spins**

$E_{\text{threshold}}$, MeV	0.1	0.2	0.3	0.4	0.7	1.5	2.0	2.5	3.0	3.5
$\nu J = 3$	5.43	5.43	5.42	5.39	3.61	2.31	1.52	0.91	0.51	0.28
$\nu J = 4$	5.82	5.81	5.80	5.75	3.60	2.20	1.42	0.85	0.48	0.26

1.2. Experimental Results Obtained at IRMM, Geel. The multiplicity method was sucessfully applied to a series of even–odd target nuclei at the 60 MeV electron linac of IRMM, Geel [6, 7]. The detection set-up consisted simply of two NaI(Tl) crystals with diameter and height both equal to 15.2 cm, placed symmetrically at 90° with respect to the neutron beam; their entrance windows were at a distance of 8 cm from the beam axis. The detectors were housed in a shielding made of lead and borated wax, while ^{10}B-slabs of appropriate thickness were inserted between sample and crystals in order to prevent scattered neutrons from

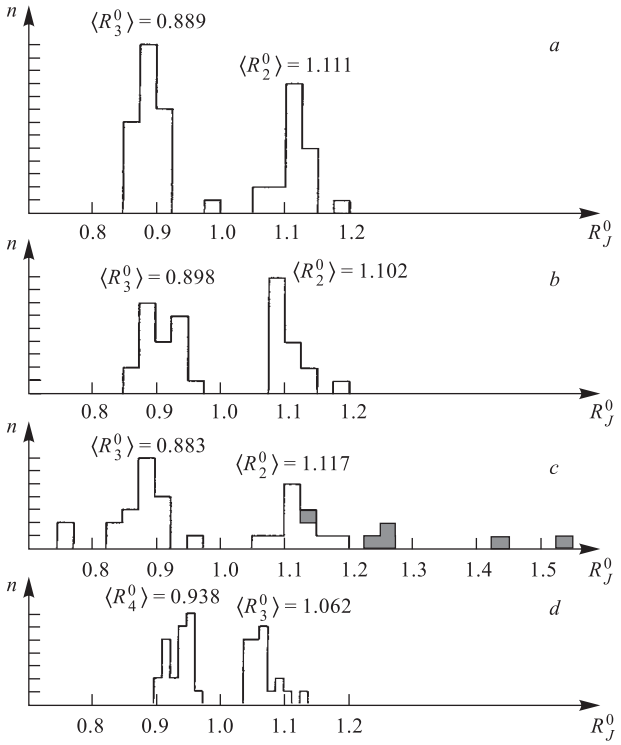

Fig. 4. Distributions of the R_J^0 values of resonances belonging to ^{105}Pd (a), ^{99,101}Ru (b), ^{95,97}Mo (c), and ^{177}Hf (d). In c, the dashed squares correspond to resonances known or suspected to be due to p-wave neutrons

reaching the detectors. Coincidences were recorded between pulses with lower threshold set at 0.3 MeV while for singles count a threshold $E_T^S = 2.5$ MeV was typically chosen. In these conditions extremely good background figures were achieved: in the case of strong resonances, values of peak-to-background ratio up to 200:1 were obtained for coincidences and 150:1 for singles. Moreover, the high detection efficiency allowed the use of a fairly long fligh path of 51 m length resulting in a relative FWHM energy resolution ranging from $1.1 \cdot 10^{-3}$ at low energy to $1.6 \cdot 10^{-3}$ at 1300 eV. Good resolution coupled to low background conditions allowed one to maximize the number of resonances measured for each nuclide.

The distributions of R_J values measured for the resonances of ^{105}Pd, ^{99}Ru, ^{101}Ru, ^{95}Mo, ^{97}Mo, and ^{177}Hf are shown in Fig. 4. For the sake of uniformity in

abscissa there are plotted, in place of R_J, the normalized values R_J^0 defined as:

$$R_J^0 = 2R_J/(\langle R_{I+1/2}\rangle + \langle R_{I-1/2}\rangle).$$

A strong grouping of R_J^0 around two different average values is evident in each case: in agreement with the results of the numerical simulations, the spin $J = I + 1/2$ is assigned to the resonances whose R_J^0 belongs unambiguously to the group with the lower value. Correspondingly $J = I - 1/2$ is assigned to the resonances of the second group.

From the data summarized in Fig. 4 two interesting conclusions can be drawn. First, in the case of Ru and Mo measurements, the values of both odd isotopes appear to group around the same averages for the two spin states so that spin assignment is possible even when the isotopic identification of a resonance is not known. Second, the Mo data exhibit a much larger dispersion than in other cases: this effect is ascribed to the presence of p-wave resonances which are strong enough to be observed since Mo falls near the peak of the p-wave neutron strength function. In order to single them out, a measurement of the relative yield of gamma rays with energy higher than 7 MeV was performed. In fact, it is expected that resonances with negative parity have a larger high energy yield than those with positive parity due to the presence of more primary $E1$ transitions. Resonances having a high energy yield more than twice that of the average for s waves are represented by dashed squares in the histogram of Fig. 4. The position in the histogram of these resonances, which are very likely p-waves,

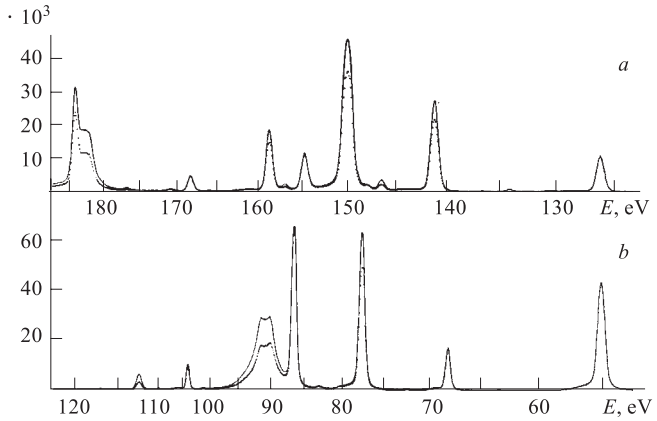

Fig. 5. Time-of-flight spectra of capture yields in Pd for incident neutron energy from 52 to 188 eV. Single counts are represented by the solid line and coincidences by the dotted line

confirms the suggestion that the large dispersion of the R_J^0 distribution observed in molibdenum is mostly due to levels with negative parity.

An example of the raw data obtained is shown in Fig. 5 where time-of-flight spectra belonging to single and coincidence counts in Pd are superposed. To display the spin effect, the coincidence counts are normalized so that resonances with $J = 3$ have the same area in singles and coincidence spectra: levels with $J = 2$ exhibit a lower coincidence yield. The effect is large enough that the spin of isolated resonances can be guessed just by visual inspection of the plot.

1.3. Experimental Results Obtained at JINR, Dubna, and Kurchatov Institute. Soon after its implementation, the multiplicity method was extensively used at the IBR-30 pulsed neutron booster of JINR, Dubna. The experimental set-up consisted of four NaI(Tl) crystals operated very much in the same way as in Geel. Spins were assigned to neutron resonances belonging to the odd isotopes of Cd, Sm, Gd, Dy, and Yb [12–17]. The distribution of R^0 values for ^{147}Sm and ^{149}Sm target nuclei is shown in Fig. 6: the separation of the values into two groups is very clear, the spin effect being about 20%.

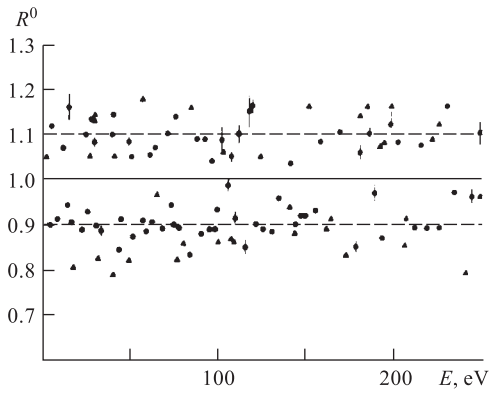

Fig. 6. Distribution of R_J^0 values for ^{147}Sm (▲) and ^{149}Sm (●) target nuclei

Several years later the method was adressed with a completely different experimental set-up, namely the 4π-multisectional detector Romashka built by G. V. Muradyan; the system was used both at the Fakel electron linac of Kurchatov Institute and at the IBR-30 of Dubna [18–21]. Many versions of this detector exist but a typical configuration consists of sixteen NaI(Tl) crystals of size $12.2 \times 12.2 \times 15.2$ cm, each one viewed by a photomultiplier. These crystals are piled up longitudinally around a vacuum pipe containing the sample. The neutron time-of-flight (TOF) and the number k of coincident gamma quanta are then recorded for each capture event so that sixteen TOF spectra, with k varying from 1 to 16, can be built. If S_k is the area under a given resonance peak for the TOF spectrum corresponding to k-fold coincidences, then the corresponding fraction of capture events is $P_k = S_k/\Sigma_k S_k$ with k running typically from 1 to 7 (higher order concidences are negligible). By plotting P_k versus k one obtains a distribution of «empirical multiplicities» which of course do not correspond to the real multiplicities of the capture process but are related to them. It was also shown that by unfolding the empirical results with an appropriate Monte Carlo code [22]

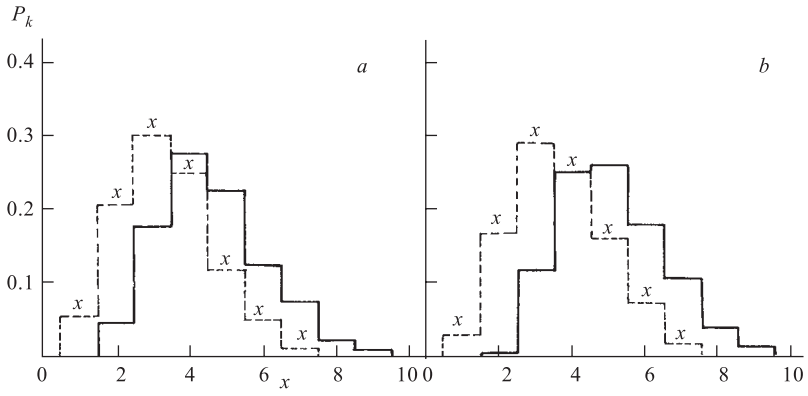

Fig. 7. Empirical (dashed line) and physical (solid line) gamma multiplicity calculated in Ref. 21 for the two spin states of ^{147}Sm (n,γ). *a*) $\langle k\rangle = 3.4$, $J = 3^-$, $\langle\nu\rangle = 4.6$; *b*) $\langle k\rangle = 3.7$, $J = 4^-$, $\langle\nu\rangle = 5.1$

which takes into account the transport of γ rays inside the detector and shielding materials, one can obtain an estimate of the real multiplicity distribution. This exercise was carried out by Georgiev et al. [21] for the target nucleus ^{147}Sm, and the results for the two spin states are shown in Fig. 7 where the dashed line represents the empirical and the solid line — the real multiplicity. For spin assignment purposes the average $\langle k\rangle = \Sigma_k(kP_k)$ was computed for each resonance and a clear grouping of these values around two different means corresponding to the two spin states is apparent.

However, the spin effect index is only about 10%, i.e., definitely less than that exhibited by the old data of Fig. 6. To conclude, Romashka is a convenient tool for estimating the multiplicity distribution of capture γ rays; moreover, it offers the advantage of simultaneously measuring, besides the multiplicity, also the total capture and scattering cross sections. However, as far as spin assignment is concerned, this detector, in its normal operating conditions, does not offer any improvement as compared to much simpler systems.

To improve this situation, Muradyan and coworkers decided to measure the multiplicity of cascades ending not only at the ground state but also at the two low-lying levels of the ground state rotational band. These states were selected by measuring the transitions de-exciting them with two thin NaI(Tl) crystals located in an internal cavity of Romashka. A detailed description of this setup is given in Ref. 19 while the results are described in Refs. 23, 24 for ^{155,157}Gd and ^{163}Dy. In this case the spin effects are much larger but they are due not so much to differences in multiplicity but rather to different populations of the low-lying

states for the two spin values. Therefore these measurements could just as well be classified in the frame of the method described in Sec. 2.

1.4. Limits of the Method. As seen in our previous sections, the multiplicity method has been very effective in providing a large number of spin assignments for a variety of nuclei. However, there are some limitations which should be taken into account. It has already been shown in Subsec. 1.1 that the spin effect index d, which is maximum for target spin $I = 5/2$, decreases with increasing I. In the case of ^{179}Hf, with $I = 9/2$, the effect is about 10%, a situation which can make the spin assignment rather problematic in view of the various sources of error, statistical and systematics, which can affect the results [25]. However, the most serious drawback of the method is that it is applicable only to even–odd target nuclei. Various experimental attempts to apply it to odd–even nuclei have all failed: in particular, no spin effect was found for the nuclei ^{115}In and ^{181}Ta, investigated in Geel [26], and for ^{165}Ho, studied in Dubna [16]. Quite unexpectedly the same situation was found for the even–odd isotope ^{171}Yb with spin $I = 1/2$. For these last two nuclei, simulations of the gamma cascade using von Egidy's code [11] confirmed the absence of spin effect. Similarly Pönitz [27] calculated the multiplicity distribution of the γ rays following s-wave capture in ^{115}In using his simulation code CASCADE which will be described later: he found that the differences due to the initial spin amount only to 1–2%.

Such a difference in the behaviour of the two classes of nuclides, even–odd and odd–even, can be explained, in our opinion, by the completely different level structure of the compound nuclei originated in neutron capture. The even–even nuclei have low-lying states of collective character which are well spaced, their excitation energies obeying to rather precise rules. It follows that even those transitions representing the last steps of the gamma cascades ending at the ground state are energetic enough to be detected by the apparatus previously described. On the contrary, odd–odd compound nuclei display a rather high density of low-lying states so that the transitions connecting those levels amongst themselves and with the ground state are often not detected either because below threshold or because internally converted. In fact, what one is actually observing is a mixture of γ-ray cascades ending not only at the ground state but also at a variety of low-lying levels of different spins. It is then no wonder that in such cases the spin effect is completely wiped out.

2. THE LOW-LYING LEVEL POPULATION METHOD

2.1. Principle of the Method. In the early days of neutron spectroscopy considerable attention was devoted to the measurement and interpretation of isomeric cross-section ratios for thermal and resonance (n, γ) reactions. In particular, Huizenga and Vandenbosch [28] tried to reproduce the available experimental data

with a simplified model of the gamma-cascade process based on the following assumptions:

a) the γ transitions are of dipole character so that the spin change at each step of the cascade is either $\Delta J = 0$ or ± 1;

b) levels of both parities are present in equal numbers so that parity changes are not followed in the cascade process;

c) the transition probabilities between levels are proportional only to the spin-dependent part of the level density of the populated states $\rho(J)$, expressed as

$$\rho(J) = \rho(0)(2J+1)\,\exp\left[-(J+1/2)^2/2\sigma^2\right]; \tag{2}$$

d) all γ-ray cascades consist of ν transitions, where ν is the average gamma multiplicity;

e) the last transition feeds the isomeric or the ground state depending on which transition has the smaller spin change.

With such simple assumptions the authors were able to approximately reproduce the experimental isomeric cross-section ratios for thermal neutron capture in a large number of nuclei by taking an average multiplicity $\nu = 3$ or 4 and values of the spin cut-off parameters σ of 3 to 5. More interesting for the purpose of the present review is the success in interpreting the results of Domanic and Sailor [29] for resonance neutron capture in ^{115}In: for such an isotope these authors found that the ratio of the high spin isomer to the low spin isomer for the 1.456 eV resonance is about 3.5 times larger than that for the 3.86 eV resonance. Calculations predict a ratio of 2.9 for $\nu = 4$ and $\sigma = 4$ if the spin of the first resonance is $J = 5$ and that of the second $J = 4$. Such spin assignments agree with those just determined by Stolovy using polarized neutrons and polarized targets [30].

Another application of the model was the interpretation of the results of Fenstermacher et al. [31] who had measured the intensity ratios of the quadrupole transitions de-exciting the $J^\pi = 6^+$ and, respectively, the $J^\pi = 4^+$ levels of the ground state rotational bands of the compound nuclei formed after neutron capture in three resonances of ^{167}Er and two of ^{177}Hf. This interpretation turned out to be not entirely correct mainly due to a rather poor resolution of the capture gamma spectra which were still obtained with NaI(Tl) crystals. However this investigation seems to us very important because the considerations previously applied to the isomeric states were extended for the first time to any other low-lying state de-excited by prompt gamma rays. This opened up the possibility of studying spin assignments or, more generally, the (n, γ) process with experimental methods belonging to the growing field of neutron time-of-flight spectrometry.

Later on, Vonach, Vandenbosch and Huizenga [32] improved the method by taking into account the energy dependence of the nuclear level density and the transition probability using the superconductor model. In 1961 Troubetzkoy [33]

published a paper concerning the calculations of the spectra of prompt γ rays following neutron capture or neutron inelastic scattering. His model was also based on the assumptions of Refs. 28, 32 but with the following modification: the levels above an energy value $E_{\rm th}$ were described by a level density formula while below this limit levels were used with parameters E, J, π known from the literature. Good agreement between the measured and the calculated γ-ray spectra was obtained.

In 1966, Pönitz [27] used a combination and an extension of the models of Troubetzkoy and of Huizenga and Vandenbosch in order to produce a simulation of the γ-cascade process able to calculate both the multiplicity distribution and the low-level populations. He used the Fermi model in order to express the energy dependence of the level density:

$$\rho(J) = (\pi^{1/2}/12a^{1/4}E^{*5/4}) \exp{(2a^{1/2}E^{*1/2})}, \tag{3}$$

where E^* is the effective excitation energy

$$E^* = E - \Delta,$$

Δ being the pairing energy.

The first and main goal of this model, which by the way is very similar to those employed in the frame of the multiplicity method, is the determination of the level density parameters a and σ and of the amount of the quadrupole contribution to the γ-ray transitions. The author however recognizes that these three values cannot all be determined from the knowledge of the isomeric ratios alone: more data are needed such as average gamma multiplicities, isomeric cross-section ratios for different spins of the initial compound state and absolute values of the population probabilities.

On the other hand, the second application of the method, consisting of the determination of the initial state spin, looks quite straightforward and capable of producing very promising results. The effect of different initial state spin on isomeric ratios or, more generally, on low-level population ratios is not only usually very large but also persists no matter how the model parameters are altered.

A similar model of the γ-ray cascade was proposed one year later by Sperber and Mandler [34, 35], who tried to reproduce various isomeric cross-section ratios by taking a set of values a and σ compatible with the literature: their conclusion was that the strength of the quadrupole radiation relative to that of the dipole radiation is enhanced as compared with that foreseen by the Weisskopf model [36, 37].

In order to display the very nature of the spin effect quite independently of any detailed calculation, we give in the following the simple description proposed by Wetzel and Thomas [37] for a generic even–even compound nucleus. Starting

from practically the same assumptions as those of Ref. 28, except for point c), these authors state that the probability of populating a low-lying level J_f after an n-step cascade is approximately proportional to the number of independent ways by which the initial state J can decay to this level under the restriction $\Delta J = 0, \pm 1$ for each step in the cascade. The underlying idea is that any proportionality factors cancel out when the population ratio R_{ab} of two final states with spins J_a, J_b formed by cascades from the same initial spin J is computed. This process is shown schematically in Fig. 8 for the example of a four-step dipole cascade from a $J = 2$ capture state to both 2^+ (solid lines) and 4^+ (dashed lines) final states. In this example, the relative population of these final states differs by a factor of two so that the ratio is $R_{42} = 0.5$.

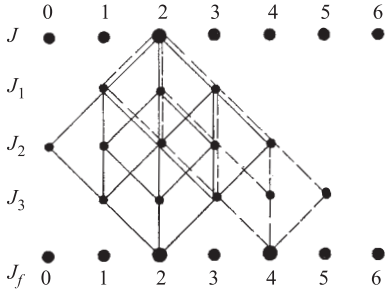

Fig. 8. Schematic representation of a four-step dipole cascade from a $J = 2$ initial state to both $J_f = 2$ (solid line) and $J_f = 4$ (dashed lines) final state

However, for $J = 3$ capture state this simplified model would clearly give equal population, $R_{42} \cong 1$ so that the ratio R_{42} is in this way strongly sensitive to J. The corresponding relative population probabilities for final states with $J_f = 0, 2, 4, 6$ formed by four-step cascades from capturing states with $J = 0$–6 are summarized in Table 2. A three-step dipole cascade would give similar results. Such a table could also be extended to final states with odd spin values which are mainly found in odd–odd compound nuclei. One may note that usually the larger the spin difference between the final states, the stronger is the dependence of their population ratio on the initial spin. The transitions to be chosen for spin assignment should conform to this rule and at the same time be strong enough and well resolved from nearby lines so that their intensities are measurable with good accuracy.

At this stage one can conclude that the present method of spin assignment is firmly established on theoretical basis, almost prior to any extensive experimental verification. However a successful application of the method depends on the positive answers to be given to the following two questions: firstly, can one always find at least two γ-ray transitions which conform to the characteristics given above? Secondly, how constant are the population ratios for resonances of a given spin? Concerning this second point, Pönitz [39] has evaluated the fluctuations around two constant values and he has concluded that they are usually very small. The only exception, in our opinion, is when the low-lying states are directly accessible from the capturing states via $E1$ transitions: in this case Porter–Thomas fluctuations of the primary γ rays can vary the populations of the low-lying states in a sizable way. If the absolute values of these primary intensities

Table 2. **Number of independent ways of populating a given level J_f from an initial state J by a four-step cascade**

J_f	J						
	0	1	2	3	4	5	6
0	3	12	6	3	1	0	0
2	6	15	19	16	10	4	1
4	1	4	10	16	19	16	10
6	0	0	1	4	10	16	19

are known, one could subtract their contribution; otherwise some fluctuations are to be expected. As regard to the first question, the final answer can only come from the experiment.

2.2. Application to s-Wave Resonances. After having been firmly established on a theoretical basis, the method was very soon applied in a number of laboratories hosting neutron time-of-flight (TOF) facilities. During a couple of years, between 1970 and 1972, there was an explosion of works on the subject produced namely at Argonne National Laboratory, Brookhaven National Laboratory, Geel Central Bureau for Nuclear Measurements, Rensselaer Polytechnic Institute, Washington Naval Research Laboratory. The decisive factor, in the widespread use of the method, was the introduction in the field of resonance neutron spectroscopy of the Ge(Li) detector which couples excellent energy resolution with reasonable efficiency.

Wetzel and Thomas [38] were the first to publish results obtained at the Argonne fast chopper facility for a number of even-Z, odd-N target nuclei. The advantage of these nuclei is that the compound nucleus formed after neutron capture decays to the ground state through collective low-lying levels including typically the well-spaced sequence of 2^+, 4^+, 6^+ rotational or 2^+, 0^+, 2^+, 4^+ vibrational states. The existence of these well-spaced levels through which the cascade must proceed also ensures that an appreciable intensity of γ rays will originate at each level. For each well resolved resonance a capture gamma spectrum was obtained and the intensity of the transitions which characterize the population probability of the selected levels was extracted. A resonance-to-resonance comparison of the intensity ratios $R_{ab} = I_a/I_b$ of the transitions de-exciting states a and b is made to investigate the spin dependence of the relative population probabilities. It should be emphasized that the ratio R_{ab} is considered since it not only suppresses any dependence of the relative populations P_a, P_b on other variables, but also eliminates the need for normalization or absolute calibration of the individual intensities I_a and I_b.

An example of the results is shown in Fig. 9, where are plotted the low-energy γ spectra of the two lowest resonances in ^{177}Hf, namely at $E = 1.10$ eV ($J = 3$)

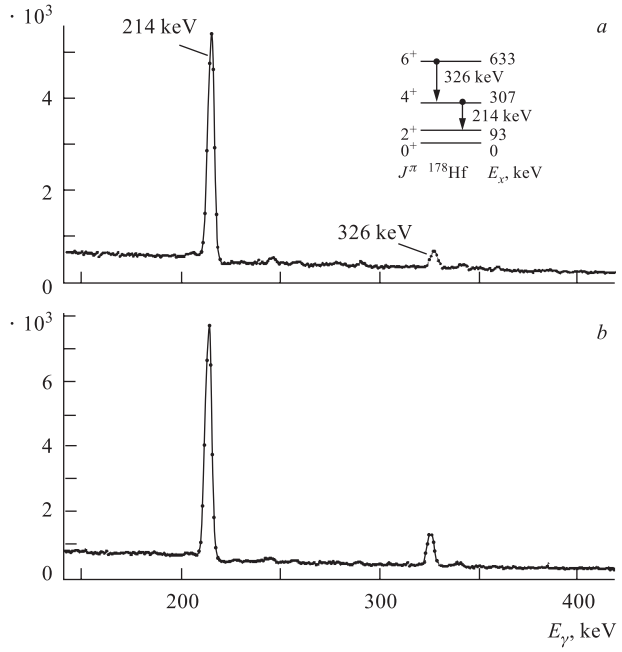

Fig. 9. A portion of the low-energy gamma spectrum in the two lowest resonances in ^{177}Hf. *a*) $E = 1.098$ eV, $J = 3$; *b*) $E = 2.380$ eV, $J = 4$

(*a*) and $E = 2.38$ eV ($J = 4$) (*b*). These spectra show one γ ray from the 6^+ level at 633 keV and one from the 4^+ level at 307 keV. The γ-ray intensities in the two spectra are normalized to the 214-keV ($4^+ \rightarrow 2^+$) line; they show that the 326-keV ($6^+ \rightarrow 4^+$) line is nearly twice as intense for the $J = 4$ as for the $J = 3$ resonance.

From the overall analysis of the data the authors conclude that the values of the ratios R_{ab} for nearly all resonances in each investgated nucleus cluster into two groups which could be associated to the two spin values of s-wave resonances. These results are also found in good agreement with previous spin assignments obtained with other methods. For each group, the average $\bar{R}_{ab}$ was calculated from which the ratio $Q_{ab} = \bar{R}_{ab}(I + 1/2)\ /\bar{R}_{ab}(I - 1/2)$ could be derived. The values of this ratio, which gives the magnitude of the spin effect, are listed in Table 3 for the target nuclei under investigation and compared with those predicted by the simple model of Table 2: the extent of the agreement between experimental and theoretical values of Q_{ab} is noteworthy in view of the simple assumptions and the elementary derivation of the predicted values. It is

Table 3. **Comparison of the experimental ratios $Q_{ab} = \bar{R}_{ab}(I+1/2)/\bar{R}_{ab}(I-1/2)$ with those predicted by the simple model of Table 2 for eight even-Z, odd-N target nuclei of spin I**

Target	I	J_a, J_b	Q_{ab} (exp.)	Q_{ab} (calc.)
^{95}Mo	5/2	4, 2	1.28 ± 0.08	1.90
^{105}Pd	5/2	4, 2	2.06 ± 0.09	1.90
^{135}Ba	3/2	4, 2	1.52 ± 0.24	1.97
^{167}Er	7/2	6, 4	1.75 ± 0.06	2.11
^{177}Hf	7/2	6, 4	1.82 ± 0.09	2.11
^{183}W	1/2	4, 2	2.06 ± 0.43	1.60
^{187}Os	1/2	4, 2	1.93 ± 0.60	1.60
^{189}Os	3/2	4, 2	1.73 ± 0.04	2.57

Note. In column 3, J_a and J_b are the spins of the relevant low-lying states.

important to stress that the spin effect may be as high as a factor of two or more, i.e., much larger than that found in the multiplicity method. Furthermore, since the nuclide in which capture takes place is identified by the specific γ rays of the product nucleus, it is not necessary that resonances in different isotopes or even contaminant elements be resolved unless they produce capture γ rays that cannot be distinguished from those of interest. However, as pointed out by the authors, there is an exception in the data of Table 3, namely the nucleus ^{95}Mo for which a Q_{ab} value as low as 1.28 ± 0.08 is measured. This finding is quite astonishing since in the case of the multiplicity method this nucleus exhibits one of the highest spin effects, namely $d = 23\%$: even if the two methods are quite different, they are based on the same general assuption that the gamma-cascade process behaves in a statistical way. A closer inspection of the data shows that the Q_{ab} value for ^{95}Mo is based only on the results of four resonances, and that the spin assigned to one of them at $E = 159.3$ eV, disagrees with that of Ref. 7. We are personally convinced that, by repeating this measurement with better TOF resolution, therefore including more resonances, such an annoying exception could be eliminated.

Odd–odd compound nuclei were first investigated by Pönitz and Tatarczuk [40] who measured low-energy γ rays from the ^{165}Ho(n,γ) reaction at the TOF facility of the Rensselaer electron linac. For this kind of nuclei it is not always known a priori whether two gamma transitions exist which de-excite two levels of appropriate spin and which are intense enough and well resolved from nearby lines to be measurable in neutron resonances. Making use of the computer code CASCADE [27], the authors were able to calculate the population probabilities for several low-lying states of ^{166}Ho and for the two possible initial spin-parity values

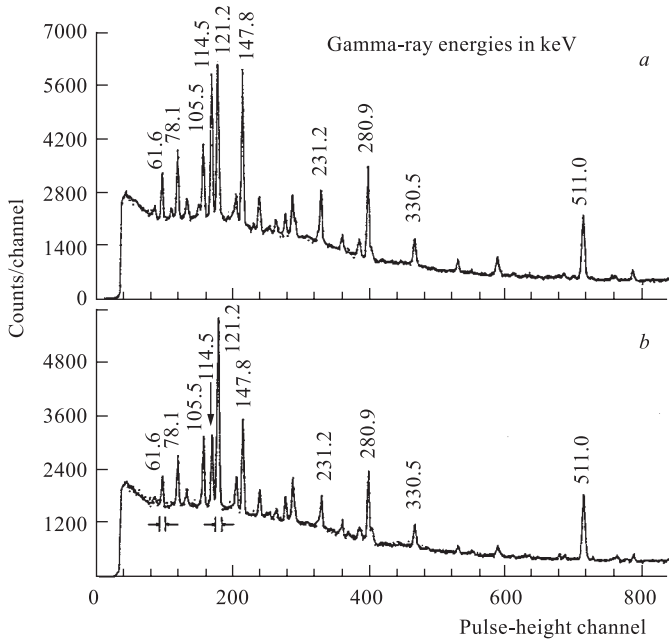

Fig. 10. Low-energy gamma spectra for 6.24 (a) and 15.4 eV (b) resonances in ^{121}Sb

$J^\pi = 3^-$ and 4^-. On the basis of this information they selected as most suitable the state at 330 keV with $J^\pi = 5^-$ and the state at 168 keV with $J^\pi = 3^-$ which are mainly de-excited by the 149 keV and the 116 keV transitions, respectively. The predicted ratio of the occupation probabilities is 0.34 for $J^\pi = 3^-$ and 0.58 for $J^\pi = 4^-$ resonance spin. In an effort to reproduce these values, the intensity ratios of the given γ rays measured for fourteen ^{165}Ho resonances were corrected for differences in photopeak efficiency, branching ratio, conversion coefficient and gamma attenuation coefficient. The agreement between experimental and theoretical values was generally good, allowing the spin determination of twelve resonances.

A more empirical approach was adopted by Bhat et al. [41, 42] in measurements of ^{121}Sb(n,γ) and ^{169}Tm(n,γ) performed at the fast chopper installed at the high flux beam reactor of Brookhaven. The low-energy γ spectra measured for nine resonances show a number of prominent γ rays, most of them below 0.5 MeV. An examination of the relative intensities of the transitions indicate that the spectra fall into two groups with respect to the intensities of the 121.2 and 114.5 keV γ rays. The spectra shown in Fig. 10 for the 6.24 eV and the 15.4 eV

resonances are characteristic of each group: one may note that the ratio of the 121.2 to the 114.5 keV peak is about 1.0 for the first resonance and 2.5 for the second one.

However, it is not possible to assign the spin to each group on the basis of these data alone since the spins of the states de-excited by such transitions are not known. In this situation one needs to know a priori the spin value of at least one resonance in each spin group: this is the case of ^{121}Sb for which the spins of the two resonances of Fig. 11 have been previously determined by Stolovy [43] using a polarized neutron beam and a polarized target.

Similarly, in the case of the target nucleus ^{169}Tm with spin $I = 1/2$, the resonances fall into two well-defined groups with respect to the relative intensities of the two prominent γ rays at 144.5 and 149.7 keV. Also here the spin effect is large with a value $Q_{ab} \cong 2$; in this case, however, the spin values of the relevant low-lying states are known, being $J^\pi = 3^+$ for the 144.5 keV and $J^\pi = 0^-$ for the 149.7 keV transition. The first γ ray is expected to be less intense in the $J^\pi = 0^+$ resonances, as the 3^+ state is farther removed from the 0^+ than from the 1^+ spin state: the spin assignment made for 13 resonances on the basis of this argument agrees, with one exception, with previous determinations based on neutron scattering measurements [44].

An interesting intercomparison of the results of the multiplicity and of the low-level population method was carried out by Coceva et al. [25] at the Geel electron linac for the target nucleus ^{179}Hf with target spin $I = 9/2$. Since for such a high spin value the spin effect d of the first method is only equal to 10%, it was felt desirable to validate the assignments with the second method which usually exhibits much larger effects.

The single-to-coincidence (S/C) values of the multiplicity method, and two different intensity ratios of the γ lines, R_1 and R_2, are displayed in Fig. 11 for the energy range 0–200 eV: a total of 44 resonances could be investigated due to the use of an isotopically enriched sample. One may notice that the R_1 values show the best separation into two groups, allowing to determine the spins of those resonances for which the multiplicity results were not conclusive. On the other hand, the higher efficiency of the first detector setup allowed the use of a flight distance of 51.6 m as compared to only 8.5 m for the Ge(Li) detector: in this way a larger number of resonances could be resolved. Also, it is sometimes useful to use more than one intensity ratio: for example, the two highest energy resonances, for which the R_1 values were not conclusive, were assigned to the two different spin groups by the R_2 results, in agreement with those of multiplicity. With one exception, i.e., the resonance at 19.1 eV, all spin assignments derived from the two methods agree.

The same approach of combining multiplicity and low-level population techniques was applied by Stolovy et al. to spin determinations of ^{143}Nd and ^{145}Nd resonances performed at the electron linac of the Naval Research Laboratory in

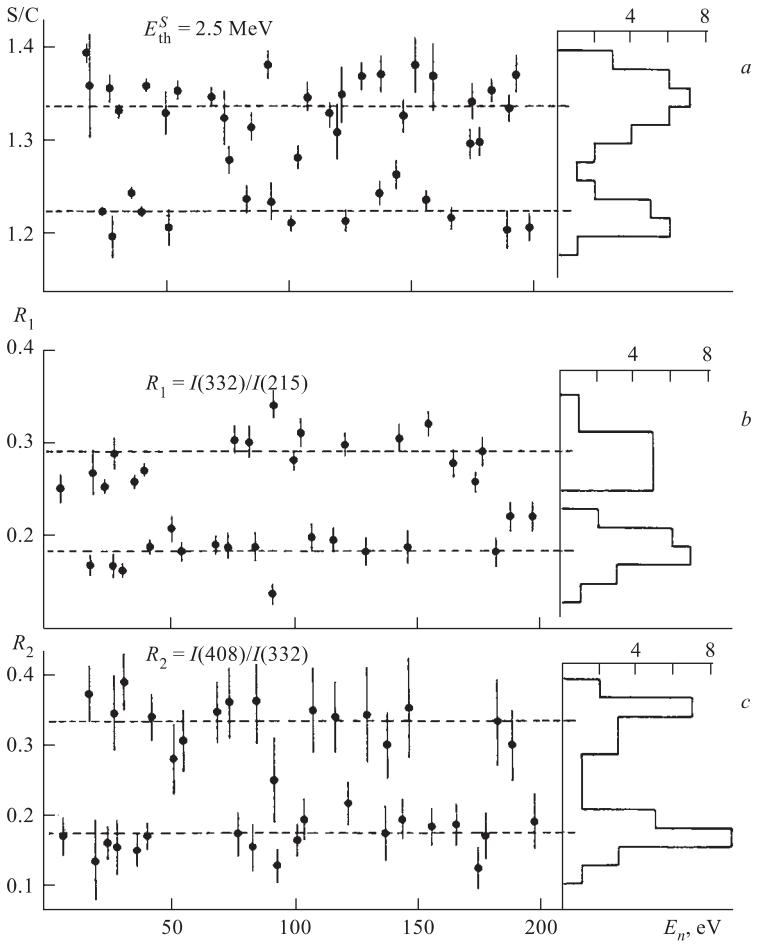

Fig. 11. Comparison of the results of the multiplicity method (a) with those of two different population ratios, R_1 (b) and R_2 (c), for ^{179}Hf (n, γ). Frequency histograms and average values are also given

Washington [45]. The authors find that the two methods complement each other nicely, except for two contradictory results, enabling to make definitive spin assignments to 18 resonances in ^{143}Nd and 29 resonances in ^{145}Nd. However from a visual inspection of the results, particularly those related to the multiplicity, one observes that many data points are scattered much more than it should be expected on the basis of their associated experimental errors. The authors ascribe such a

scattering to Porter–Thomas (PT) fluctuations and present a maximum likelihood method to estimate them: the final outcome is that, for each resonance, a «probability of correctness of the spin value» is calculated. If this indicator is larger than 90%, the spin is assigned. Personally we find surprising that such large PT fluctuations exist for nuclei of high level density such as those under investigation; however the method may be useful in order to quantify variations probably due to a number of systematic uncertainties which are difficult to estimate otherwise.

An important result obtained in Geel was the successful spin determination of fourteen ^{235}U resonances [46]. The application of the low-level population method to a fissile nucleus such as ^{235}U is hindered by two major difficulties: (i) the presence of prompt and delayed fission γ rays and (ii) the natural γ activity of the sample.

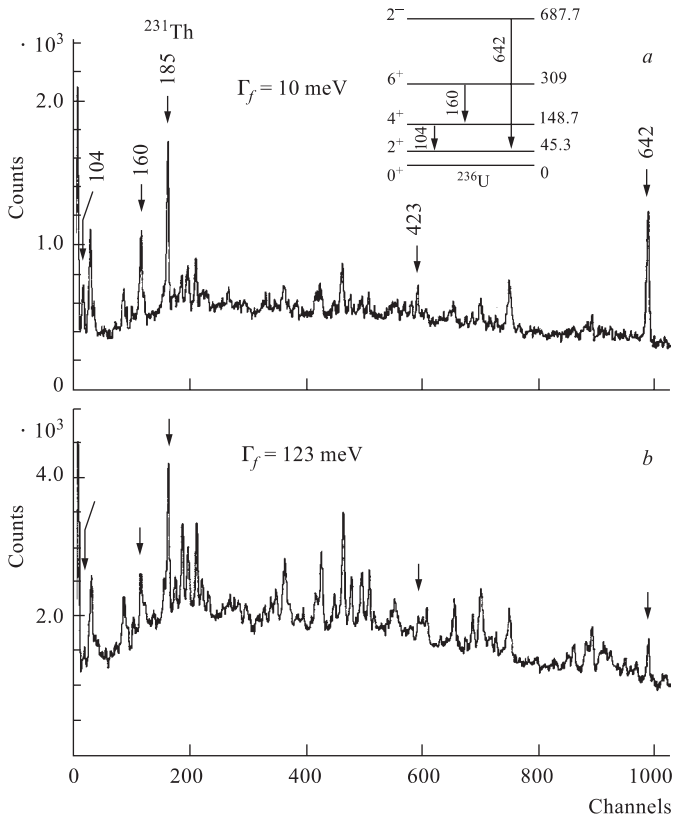

Fig. 12. Two low-energy gamma-ray spectra from the 6.39 (*a*) and 8.79 eV (*b*) resonances of ^{235}U. The peaks at 104, 160, 423, and 642 keV are capture gamma-rays

The first effect highly complicates the structure of the low-energy gamma spectra emitted from ^{235}U resonances, while the natural activity is strong enough, compared with the available sources of resonance neutrons, to wipe out any other effect below about 250 keV. In order to remove most of this activity, a coincidence measurement was performed involving a Ge(Li) detector and a large 18×15 cm NaI(Tl) crystal: pulses from the Ge(Li) were accepted only when in coincidence with pulses from the NaI(Tl) corresponding to energies higher than 0.7 MeV. In this way the γ activity should be removed except for random coincidences. Two low-energy spectra obtained for the resonances at 6.39 and at 8.79 eV, respectively, are shown in Fig. 12.

In the upper spectrum, which corresponds to a resonance with predominance capture, are clearly visible the capture peaks at 104, 160, 423, and 642 keV and the main activity peak at 185 keV, still visible because of random coincidences. The relevant ^{236}U level scheme is represented above. The remaining structure is mainly due to fission γ rays as it appears from a comparison with the spectrum in the lower half, referring to a resonance with predominant fission. The transitions at 642.4 keV, de-exciting a 2^- state, and at 160.3 keV, de-exciting the 6^+ member of the ground state rotational band, were selected for spin assignment. A refined shape analysis based on a generalized shape fitting method was necessary in order to derive the intensity of the 160.3 keV line which overlaps with an activity peak at 163.3 keV and with a fission peak at 158.8 keV. Fits of this triplet and of the peak at 642.4 keV are plotted in Fig. 13 for six assigned resonances. The height of the bar below each peak is proportional to its intensity: one assigns spin $J = 4$ when the bars of the 160.3 and 642.4 keV have approximately equal height, and spin $J = 3$ when they are in a ratio of about $1 : 2$. In fact the large spin difference of the two de-excited low-lying states is very favourable for the method, giving a spin effect $Q_{ab} = 2.2$. Because of the presence of the partially unresolved fission γ ray at 158.8 keV, the results were considered reliable only for fourteen resonances with fission widths $\Gamma_f \leqslant 50$ meV. All these spin determinations were confirmed a year later by the work of Keyworth et al. who assigned the spins of 65 resonances using polarized neutrons and polarized target in the frame of a collaboration between Oak Ridge and Los Alamos laboratories [47].

In Geel, the method was also applied to the target nucleus ^{115}In, resulting in the assignment of 31 resonances of this isotope [48]. The main reason for this work was the interpretation of the primary γ rays following resonance neutron capture in ^{115}In: if the reduced widths of these transitions averaged over resonances of the same spin are known, then information on spins and parities of the corresponding low-lying states can be derived.

As an extension of the work of Ref. 40, spins were assigned in Geel [49] also to an unusually long string of resonances, namely 64, belonging to the ^{165}Ho target nucleus. In the same paper an original method is presented allowing one to extend the measurement of the s-wave neutron strength function per spin state to

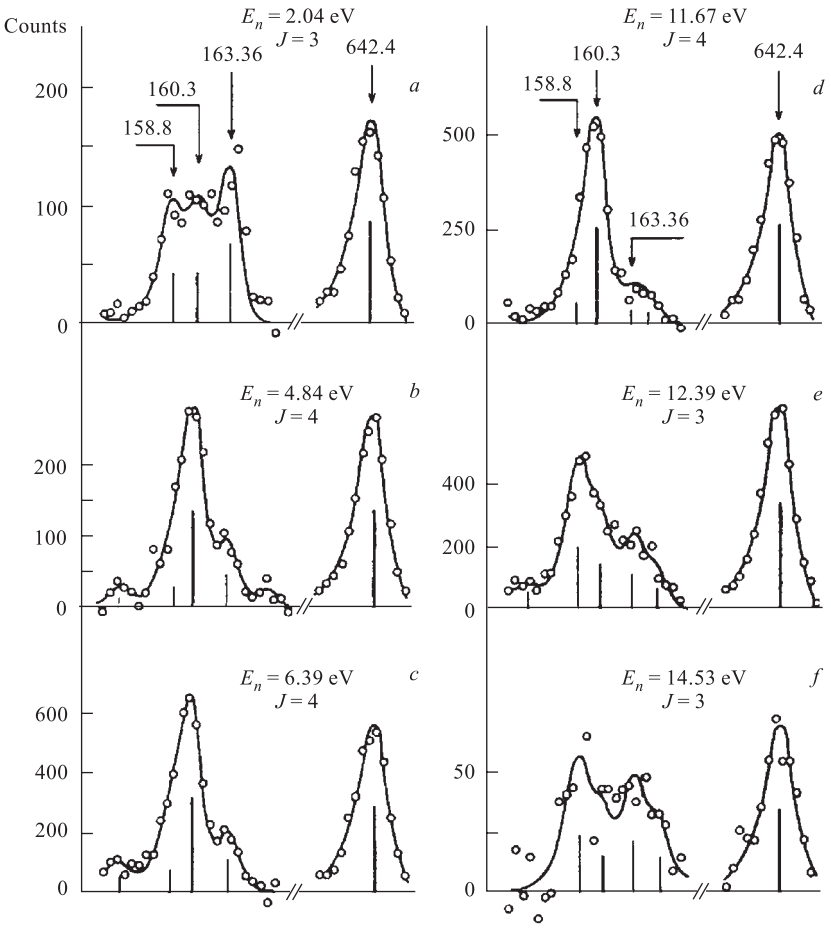

Fig. 13. Fitted spectra for 154–169 keV energy region plotted together with 624.2 keV peak for six ^{235}U resonances to which spin was assigned. 624.4 keV peak is reduced by a factor of two for better comparison

the region of the unresolved resonances. This method is based on the expectation that, when dealing with a neutron-energy interval containing more resonances of both spins, the resulting population ratio of two appropriate low-lying states takes up an intermediate value between those corresponding to $J = I + 1/2$ and $J = I - 1/2$ capturing states, depending on the number and strength of the resonances of each spin. This suggests that, after suitable calibrations, the measurement of population ratios can be used to deduce the neutron capture rate

Table 4. **Experimental ratios $Q_{ab} = \bar{R}_{ab}(I+1/2)/\bar{R}_{ab}(I-1/2)$ for eight odd-Z target nuclei of spin I**

Target	I^π	J_a^π, J_b^π	Q_{ab} (exp.)	References
^{115}In	$9/2^+$	5^+, 2^+	2.10	[48]
		5^+, 3^+	2.37	[48]
^{121}Sb	$5/2^+$	4^-, 1^+	2.57 ± 0.33	[51]
^{159}Tb	$3/2^+$	4^-, 1^+	1.92 ± 0.28	[51]
		4^-, 0^+	1.88 ± 0.27	[51]
		4^-, 1^-	1.69 ± 0.24	[51]
		3^+, 0^+	1.50 ± 0.14	[51]
^{165}Ho	$7/2^-$	5^-, 2^+	1.97 ± 0.19	[51]
		6^+, 2^+	1.67 ± 0.13	[51]
		5^-, 3^-	1.63 ± 0.22	[51]
^{169}Tm	$1/2^+$	3^+, 0^-	2.11 ± 0.36	[42]
^{175}Lu	$7/2^+$	5^+, 1^-	1.89 ± 0.04	[50]
^{176}Lu	7^-	$13/2^-$, $9/2^-$	1.27 ± 0.02	[50]
^{181}Ta	$7/2^+$	4^+, 1^-	1.38 ± 0.21	[51]
		4^+, 2^+	1.37 ± 0.19	[51]
		4^+, 2^-	1.31 ± 0.13	[51]

Note. In column 3, J_a^π and J_b^π are the spins and parities of the relevant low-lying states.

(and thus the strength function) per spin state at energies where the resonances cannot be resolved. Applying of this method to ^{165}Ho has resulted in strength function values with statistical uncertainties considerably lower than those derived from resolved resonances alone, as apparent from the data of Table 7 in Sec. 3.

Low-energy γ rays from resonance neutron capture in ^{175}Lu and ^{176}Lu nuclei were measured by Aldea et al. [50] at the Pulsed Fast Reactor IBR-30 of Dubna, operated in a booster mode in conjunction with the electron linac LUE-40. Spins were assigned to a number of resonances in both isotopes: particularly noteworthy are the results obtained for the rare odd–odd nucleus ^{176}Lu with spin and parity 7^-, showing that the method is applicable also to very high target spin values.

In Dubna, Olejniczak et al. [51] concentrated recently on determining the spin effect for a number of odd–odd compound nuclei. Their results are summarized in Table 4 which is the equivalent of Table 3 for the class of odd-Z target nuclei: the only differences being that, for a given isotope, several pairs of low-energy transitions are studied while no comparisons with calculated values are given. For the sake of completeness, the table includes also results of previous works. An inspection of the table shows that, with the possible exception of ^{176}Lu and

^{181}Ta, the values of the spin effect are of the same order as those of the even–even compound nuclei. Moreover, since the spectra are more complex, there are usually several transitions which can be used for spin assignment purposes.

Before ending the present section, we would like to mention an extension of the method which is important although not directly relevant to the subject of the present review. We refer to the use of the population technique to determine the spins of the final bound levels instead of those of the initial states. This development, which was carried out by Coceva et al. in Geel [52] and by Breitig et al. in Brookhaven [53], is based on the following straightforward idea: since the population P_a of a given state a depends, amongst other things, both on its spin and on that of the initial state, one can reverse the procedure used for the spin assignment of neutron resonances in a completely specular way. More precisely, the spin J of a final state a can be derived from the value of the ratio $R_a = P_a(+)/P_a(-)$ where numerator and denominator are the population of level a following capture in an s-wave resonance with spins $I+1/2$ and $I-1/2$, respectively. Clearly, in the experimental procedure, the population values are also in this case replaced by the intensities of the relevant γ transitions.

The main difference as compared to the previous application is that, while s-wave resonances have only two possible spins, the final bound levels have a variety of spin values. However, in applying the method to the compound nuclei ^{106}Pd and ^{178}Hf, Coceva et al. were able to show that the dependence of R_a on J is strong enough to allow distinction of up to six different spin values. Clearly the actual spin assignment of bound levels requires, besides the experimental data, also an accurate simulation of the γ-cascade process: this was performed both with an analytical and with a Monte Carlo method with satisfactory results.

To conclude, the low-lying level population method has met since the beginning with a considerable success: first of all, different from the multiplicity method, the present one is applicable to any kind of compound nucleus, whether even–even or odd–odd. Secondly, the spin effects Q_{ab} are large, reaching easily a factor-of-two difference in the intensity ratios R_{ab}, as apparent from the data of Tables 3 and 4. Moreover, these ratios are rather constant for a given spin so that a clear clustering around two different averages is always achieved. Finally, the success in determining also resonance spins in a fissile nucleus shows the capabilities of the method in discriminating against spurious effects.

There is however also a reverse of the medal. The use of Ge(Li) detectors of limited efficiency and the need to collect gamma spectra of reasonable statistics belonging to individual resonances has forced experimenters to use short flight paths thus restricting the number of resonances which could be resolved. Even so, collecting sufficient counts in weak resonances has been a problem, particularly when only limited quantities of isotopically enriched samples were available. Because of these experimental difficulties the main objective of several papers has been to establish a new method rather than to determine those long sequences

of resonance spins which are needed in order to study the spin dependence of the nuclear quantities which are referred to in the Introduction. Even when the experimental conditions improved because of the advent of more powerful pulsed neutron sources and of the large coaxial Ge-detectors nowadays available, there was not that expansion of the field which could have been possible and desirable. It follows quite paradoxically that the longest strings of spin-assigned resonances were usually obtained with the multiplicity method even if this technique is definitely less performing that the low-level population method.

2.3. Application to p-Wave Resonances. There has been a revival of spin determinations in the last ten years in relation to parity nonconservation (PNC) measurements in neutron resonances. Parity nonconservation, a property of the weak interaction, is strongly enhanced in $l = 1$ neutron resonances due to the small level spacing and the large ratio of the neutron widths of s wave compared to those of p-wave neutron resonances [54, 55]. Whereas the ratio of the strength of the weak to that of the strong interaction is about 10^{-7} in the nucleon–nucleon interaction, this enhancement may easily produce PNC effects of several per cent in compound nucleus reactions [56]. Such effects were investigated by the TRIPLE collaboration by measuring the longitudinal asymmetries $P = (\sigma_+ - \sigma_-)/(\sigma_+ + \sigma_-)$ in p-wave neutron resonances where σ_+, σ_- are the p-wave resonance cross sections for neutron spin parallel, respectively antiparallel to the neutron momentum. Such studies were carried out at the LAMPF/LANSCE pulsed neutron facility of Los Alamos National Laboratory by measuring the transmission of polarized neutrons through unpolarized targets of ^{238}U and ^{232}Th. Significant parity nonconservation effects were found in several resonances of these isotopes allowing to estimate for the first time the root mean squared PNC matrix element M in nuclear matter, a quantity that reveals the overall effective strength of the weak interaction in the nucleus [57–60]. In a second time, the attention was turned to the mass region around $A = 110$ where the maximum of the $3p$ neutron strength function is situated: isotopes such as ^{106}Pd, ^{108}Pd, ^{107}Ag, ^{109}Ag, ^{113}Cd, and ^{115}In were studied [61–64].

This helicity dependence of the total cross section originates from the mixing of compound states of same spin but opposite parity: it is then clear the importance of knowing the resonance spins in order to interpret and to check the PNC results. In this respect it is convenient to distinguish two types of target nuclei: first the zero-spin nuclei such as ^{238}U and ^{232}Th, for which only $p_{1/2}$ resonances can mix with $s_{1/2}$, and therefore exhibit PNC effects, while $p_{3/2}$ resonances cannot. In the case of ^{238}U it has been shown that the knowledge of the spins of $l = 1$ resonances improves the estimate of the root mean squared PNC matrix element M only in a very limited way. However the spin assignments have, in our opinion, the important function of checking and hopefully confirming the parity nonconservation measurements by verifying that all resonances showing significant PNC effects have the right spin. On the other hand, for nonzero spin

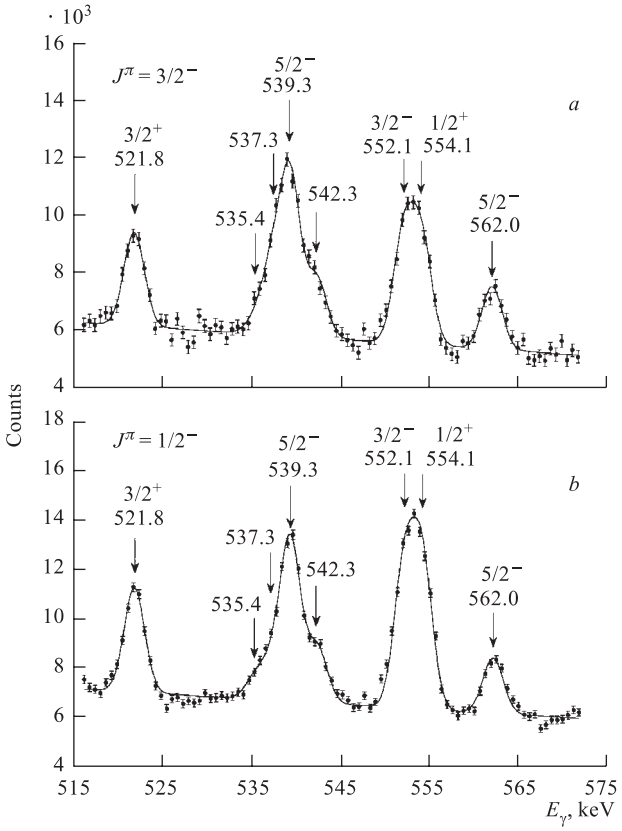

Fig. 14. Example of a fit of the capture gamma-rays spectra in the 515–575 keV region for ^{238}U p-wave resonances at 10.24 (a) and 89.24 eV (b)

target nuclei the knowledge of the spins of both s- and p-wave resonances is of primary importance for an accurate determination of the r.m.s. matrix element M: in absence of such information one can proceed by averaging but this usually introduces a large uncertainty in the value of such a quantity.

Extension of the low-level population method to p-wave resonances is straightforward though experimentally much more difficult because of the very weak strengths of most p-wave as compared to s-wave resonances at epithermal neutron energies. The measuring time can span over several weeks if not months and special care must be taken in estimating background corrections particularly in the presence of resonance overlapping. An additional complication is the fact that p-wave resonances may have up to four different spin values, depending on

the spin of the target nucleus, so that the method must be able to clearly separate up to four resonance groups. In this respect however the success obtained in determining the various spins of the final bound states looks very promising [52].

Results obtained at Geel for the target nuclei ^{238}U,^{113}Cd, ^{107}Ag, ^{109}Ag, and ^{115}In are summarized in the following [62, 64–68]. Sections of the γ-ray spectra belonging to the two most intense ^{238}U p-wave resonances at 10.24 and 89.24 eV are shown in Fig. 14.

At the top of each peak the energy and the spin and parity of the relevant de-excited state are shown. One may notice that in the upper part of Fig. 14 the doublet dominated by the 539 keV line, from a $5/2^-$ state, is higher than the multiplet at 552–554 keV, de-exciting states with $J^\pi = 1/2^+, 3/2^-$. In the lower part the opposite is true. As a consequence $J^\pi = 3/2^-$ was assigned to the 10.24 eV resonance; and $J^\pi = 1/2^-$, to the 89.24 eV resonance.

The ratios R of the intensities of the two doublets $R = (I_{537} + I_{539})/(I_{552} + I_{554})$ are plotted in Fig. 15 for fourteen p-wave resonances: a clear splitting into two groups is apparent, allowing the spin assignment of all investigated resonances [65, 66]. For a few $p_{3/2}$ resonances, these data agree with the spin information derived from primary gamma rays.

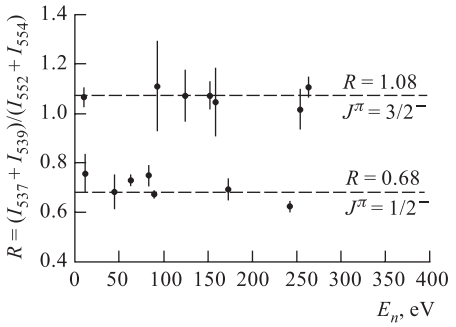

Fig. 15. The ratio R between the sums of the intensities of the identical gamma rays plotted versus the energy of fourteen ^{238}U p-wave resonances

There is a general consistency between these spin assignments and the values of the longitudinal asymmetry P obtained in the later and more accurate measurement of the TRIPLE [59]: the five p-wave resonances showing significant PNC effects, i.e., having $P/\delta P > 5$, namely those at 11.31, 45.17, 63.52, 89.24, and 173.18 eV, have all been assigned $J = 1/2$. However, as anticipated, the estimate of the r.m.s. PNC matrix element is little influenced by the spin knowledge: the values with and without spin information are respectively

$$M = 0.67^{+0.24}_{-0.16} \quad \text{and} \quad M = 0.69^{+0.26}_{-0.17} \text{ meV}.$$

In the case of the target nucleus ^{113}Cd, with groundstate spin and parity $I^\pi = 1/2^+$, p-wave resonances with $J^\pi = 0^-$ and 1^- can mix with $J^\pi = 0^+$, respectively $J^\pi = 1^+$ s-wave resonances, while p resonances with $J^\pi = 2^-$ cannot exhibit any PNC effect. In addition, in the case of the measurement of longitudinal asymmetries, parity mixing requires not only the same spin, but also

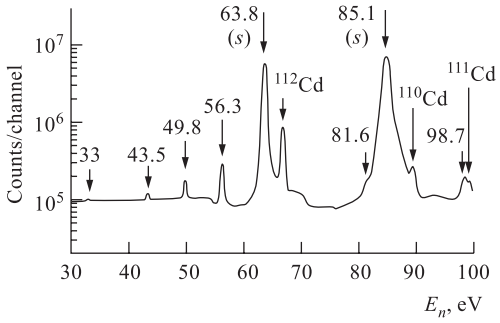

Fig. 16. Part of the time-of-flight spectrum for ^{113}Cd(n,γ) on a log scale with the resonance energies indicated

the same total neutron angular momentum at the entrance channel $\mathbf{j} = \mathbf{l} + \mathbf{s}$ [56, 69]. It follows that for p-waves with $J = 1$, only the $p_{1/2}$ fraction of the neutron entrance channel can mix with the corresponding s-wave resonance. Since this fraction is usually unknown, this contributes an additional uncertainty to the final result.

Part of the time-of-flight spectrum representing the total number of γ-ray pulses observed in the Ge-detector and corresponding to $E_\gamma > 0.3$ MeV, is plotted in Fig. 16 as a function of neutron energy for the reaction ^{113}Cd (n,γ): one may notice how weak are the p-wave resonances as compared to the two large s waves at 63.8 and 85.1 eV.

Low-energy γ-ray spectra in the 525–850 keV region are plotted in Fig. 17 for three p-wave resonances to which different spins have been assigned.

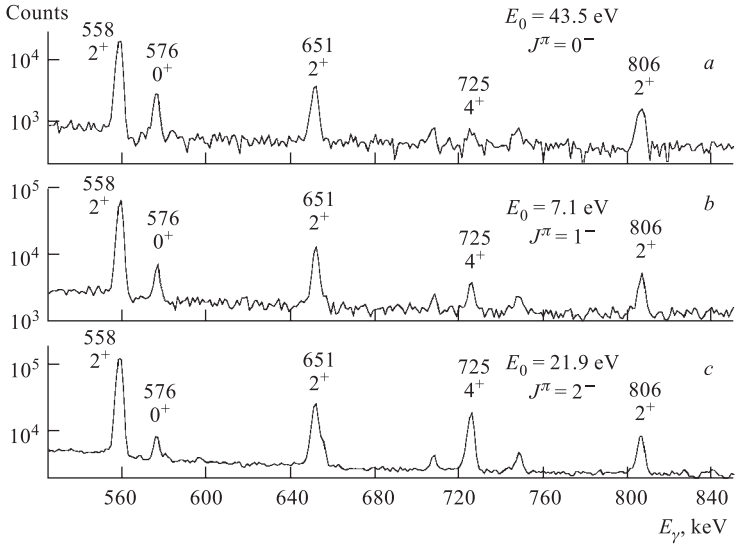

Fig. 17. Capture gamma-rays spectra for the first three p-wave resonances of ^{113}Cd having different spin

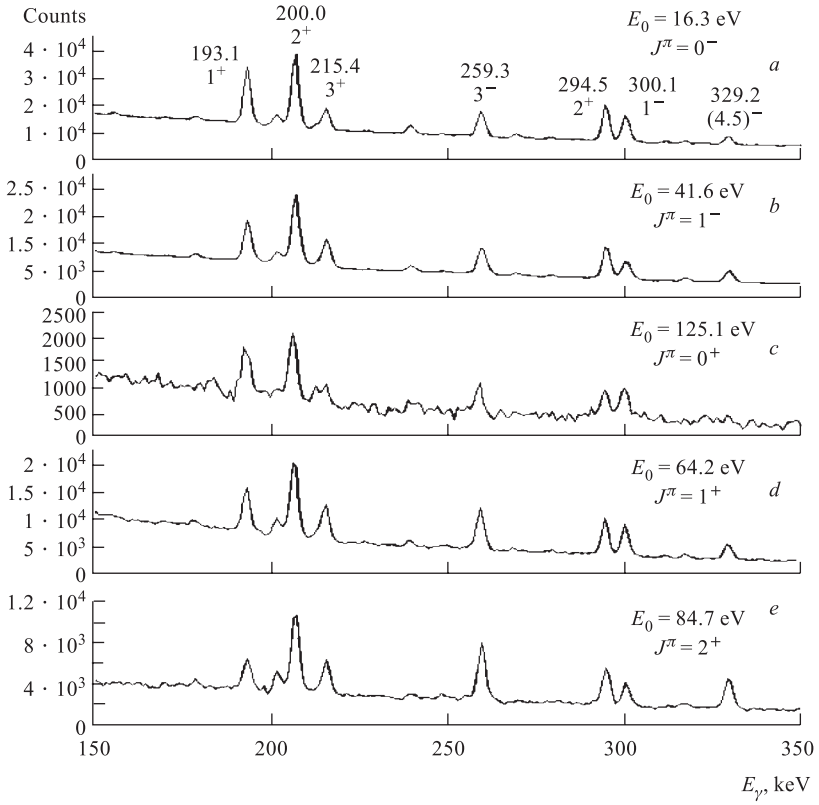

Fig. 18. Low-energy gamma-ray spectra for five ^{107}Ag resonances of different spin and parity: the energies of the strongest transitions and the spins and parities of their initial levels are indicated

The intensity of the strong 558 keV transition can be considered in first approximation as a measure of the number of neutron captures, quite independently of the spin, since about 70% of all decays pass through this first excited 2^+ state. Compared to that, the intensity of the 725 keV transition, from a 4^+ level, increases with the resonance spin value. The intensity ratio of these two lines has been used to assign the spin to 21 p-wave and 23 s-wave resonances: these data have been used by the TRIPLE Collaboration [61], for determining the r.m.s. PNC matrix element M for ^{113}Cd.

The computer code DICEBOX [70] was used to simulate the process of statistical gamma cascade de-excitation of ^{113}Cd [71]. The program generates sets of levels in the quasi-continuum region of the excitation spectrum according to a

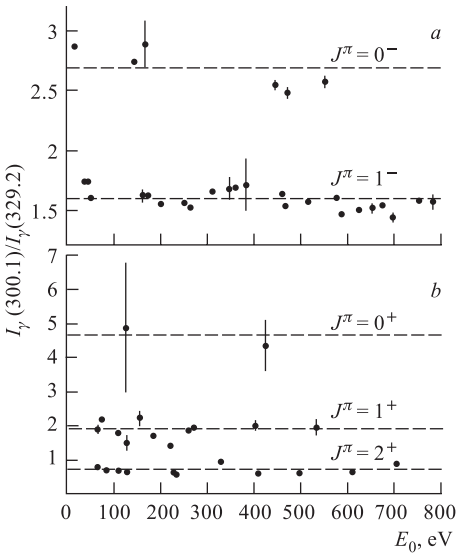

Fig. 19. Intensity ratios between the indicated gamma-ray transitions plotted versus neutron energy for ^{107}Ag resonances: *a*) s-wave resonances with $J = 0$ and 1; *b*) p-wave resonances with $J = 0$, 1, and 2. The dashed lines are the means of the various groups

given level-density formula and generates also a corresponding full set of partial radiative widths. An event consists of the gamma decay of the highly excited resonance state through intermediate levels to a level in the discrete region. In this way, the population of these levels is simulated. The event-by-event basis of the program allows a rigorous inclusion of the Porter–Thomas fluctuations of the individual γ-ray intensities. The results of these simulations are in excellent agreement with the experimental data.

The odd target nuclei ^{107}Ag and ^{109}Ag have spin and parity $I^\pi = 1/2^-$, therefore the same considerations already expressed for ^{113}Cd apply as far as PNC effects are concerned. Low-energy γ-ray spectra for five resonances of different spin and parity are shown in Fig. 18.

The energies of the stronger transitions are indicated, along with the spin and parity of the state from which the transition originates. One may note that the intensities of the transitions at 215.4, 259.3, and 329.2 keV, depopulating levels with spin ranging from 3 to 5, increase with the resonance spin value. The opposite happens for transitions at 193.1 and 300.1 keV, depopulating levels with $J = 1$.

The intensity ratios between the γ-ray transitions at 300.1 and 329.2 keV are plotted in Fig. 19 versus the energy of the ^{107}Ag s- and p-wave resonances.

The separation into two and three spin groups, respectively, is distinctive, allowing a clear-cut J assignment. From the values of the longitudinal PNC asymmetries measured by the TRIPLE Collaboration for 15 p-wave resonances, it was possible to calculate the most probable value of the r.m.s. PNC matrix element M_J separately for the two spin groups [62]. Maximum likelihood plots are shown for $J = 1$ and $J = 0$ in Fig. 20. The $M_{J=0}$ value for ^{107}Ag has a large uncertainty because it is obtained from only three PNC effects. Nevertheless, the M_J values for ^{107}Ag appear to demonstrate for the first time a J dependence of M_J.

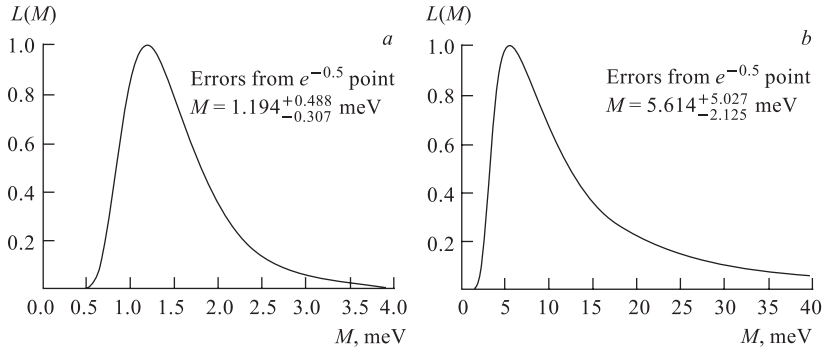

Fig. 20. Maximum likelihood plots for $J = 1$ (a) and $J = 0$ (b) resonances in ^{107}Ag

The spreading width of the weak interaction is defined as $\Gamma_w = 2\pi M_J^2/D_J$. Assuming that this width is independent of J, a likelihood analysis was performed including the data from both spins simultaneously: a value $\Gamma_w = (4.93)^{+3.43}_{-1.87} \cdot 10^{-7}$ eV was obtained. Repeating the same exercise without introducing any spin information yielded: $\Gamma_w = (11.19^{+12.0}_{-5.48}) \cdot 10^{-7}$ eV.

Comparison of these figures proves beyond any doubt the enormous influence of the spin information on the estimates of the weak spreading widths.

Similar results have been obtained for ^{109}Ag except that in this case no PNC asymmetries have been measured for $J^\pi = 0^+$ resonances. Therefore the likelihood analysis was performed only on the sample of $J^\pi = 1^+$ resonances, yielding a value:

$$\Gamma_w = (1.30)^{+2.49}_{-0.74} \cdot 10^{-7} \text{ eV}.$$

These data are described in detail in Refs. 62, 67, 68.

Finally spins were assigned to the resonances of the ^{115}In target nucleus with spin and parity $I^\pi = 9/2^-$: in this case s-wave resonances have $J^\pi = 4^+$, 5^+ while p-wave resonances have $J^\pi = 3^-$, 4^-, 5^-, and 6^-. Spin assignment of s-wave resonances has already been reported [48] so that in recent papers [64, 67] the main emphasis was put on the investigation of p-wave resonances. Low-energy gamma-ray spectra are given in Fig. 21 for five different spin and parity combinations.

Because of their large intensities it is convenient to use for spin assignment the 186.2 keV transition de-exciting a 313.5 keV level with $j^\pi = 4^+$, 5^+ and the 273.0 keV transition de-exciting a level of the same energy with $j^\pi = 2^+$. The ratios of the corresponding intensities are plotted versus neutron energy in Fig. 22 for s- and p-wave resonances together.

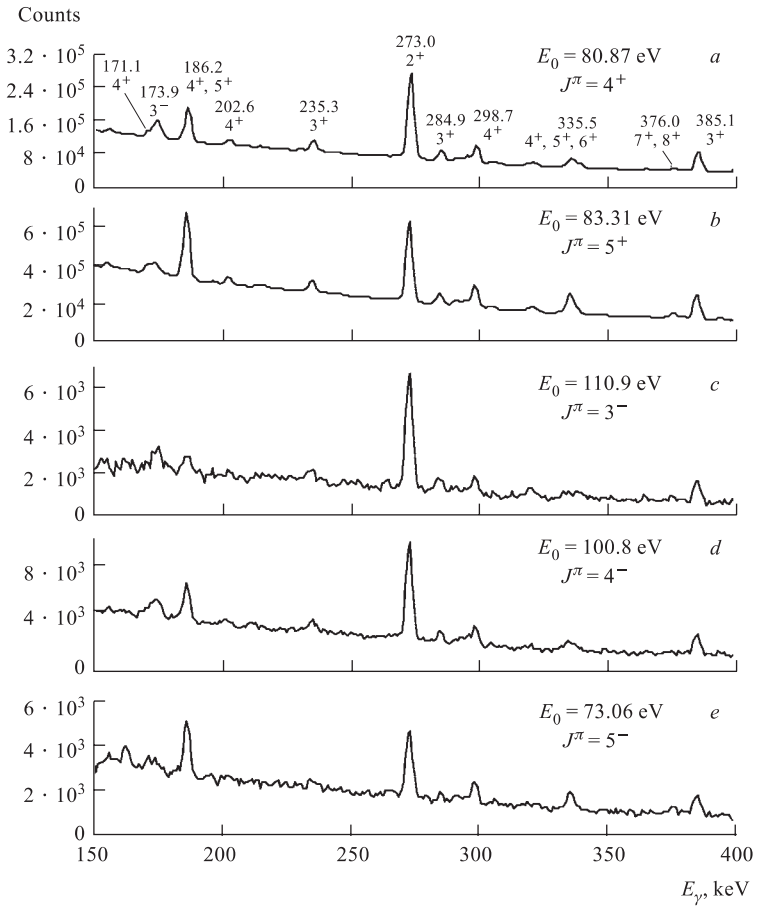

Fig. 21. Low-energy gamma-ray spectra for five ^{115}In resonances of different spin and parity

The lowest group, with ratios around 0.1, contains only p-wave resonances which are identified as having $J^\pi = 3^-$. A second group having values around 0.4 and containing resonances of both parities, is identified as $J = 4$. There is finally a third group showing wider fluctuations of the ratios around a value of 0.8 and containing both s-wave and p-wave resonances. In Ref. 64 these were identified as having all $J = 5$. If this were the case, it would mean that out of a sample of twenty four $l = l$ resonances, twelve have $J^\pi = 5^-$ and none has $J^\pi = 6^-$. Since this situation is highly unlikely, we suggest that the higher

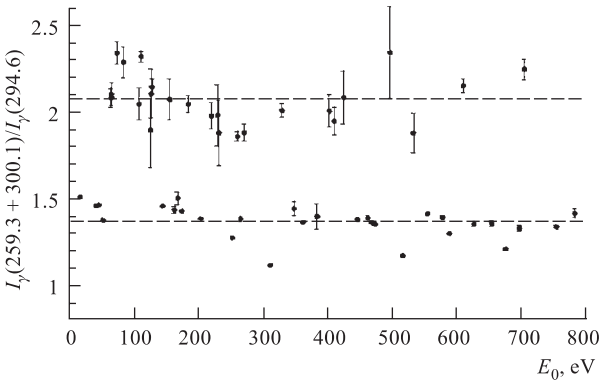

Fig. 22. Intensity ratios between the indicated gamma-ray transitions plotted versus neutron energy for s-wave (■) and p-wave (●) resonances in ^{115}In

group contains both $J^\pi = 5^-$ and $J^\pi = 6^-$ p-wave resonances and that the chosen intensity ratio is unable to distinguish amongst them. Unfortunately, in view of the weakness of the most p waves, it is not possible to use intensity ratios belonging to other transitions because of insufficient statistics.

Likelihood analysis based on the longitudinal asymmetries measured by the TRIPLE was performed in order to determine the best estimate of the weak spreading width. The results obtained with and without spin information are respectively:

$$\Gamma_w = (1.303^{+0.761}_{-0.429}) \cdot 10^{-7} \text{ eV} \quad \text{and} \quad \Gamma_w = (1.407^{+1.321}_{-0.581}) \cdot 10^{-7} \text{ eV}.$$

2.4. Application to Parity Assignments. Although the subject of this section is strictly speaking not in keeping with the scope of the present review, it is convenient to briefly deal with it since it is a natural extension of the low-level population method.

In fact, the nonspecialist reader could wonder how the parity of the resonances investigated in the previous section was assigned. The standard method to determine the orbital angular momentum of a low-energy neutron resonance is based on its neutron width and uses the Bayes' theorem on conditional probability [72] as developed by Bollinger and Thomas [73]. This method relies on the fact that the difference in penetrabilities for the s- and p-wave is so large that most of the weaker resonances are p wave and most of the stronger resonances are s wave. In practice this method works well for most nuclei at low neutron energy but tends to give ambiguous results with increasing energy, due to the overlapping of the two neutron width distributions. In order to check these

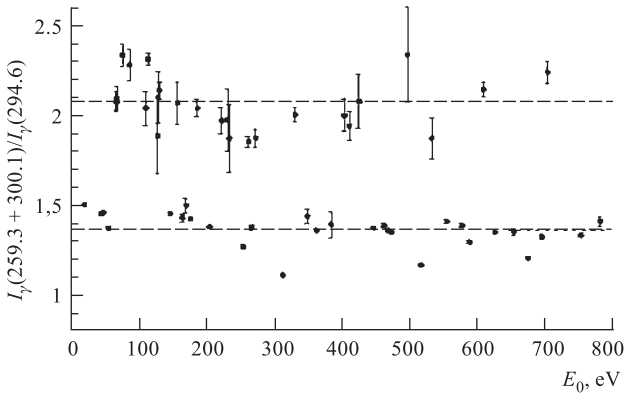

Fig. 23. Intensity ratios between the indicated gamma-ray transitions plotted versus neutron energy for s-wave (■) and p-wave (●) resonances in ^{107}Ag. The dotted lines are the means of the two groups

assignments which are based solely on statistical arguments, it is interesting to investigate whether the radiative decay patterns show a «parity» effect analogous to the «spin» effect previously described. This study was carried out for two odd isotopes of silver [62, 67, 68]. In an attempt to separate the ^{107}Ag resonance sample into two groups, with $l = 0$ and $l = 1$, the ratio was considered of the sum of the intensities for the two transitions at 259.3 and 300.1 keV, de-exciting negative parity states, and the intensity of the 294.6 keV transition, de-exciting a positive parity state (see Fig. 18). This intensity ratio is plotted in Fig. 23: a net separation is evident between the two parities. The value $l = 0$ is assigned to the lower group and $l = 1$ to the upper group. Lacking any theoretical guidance, this assignment is justified from the fact that all resonances with higher values of $g\Gamma_n$, and therefore certainly s wave, are in the lower group. These assignments agree with those obtained from the Bayes' theorem except in three cases: however the three concerned resonances have neutron widths intermediate between the s-wave and p-wave group, so that statistical methods cannot provide for them a definite and reliable answer. Very similar results were obtained for ^{109}Ag.

The most astonishing in the data of Fig. 23 is that, by chosing an appropriate intensity ratio, such a separation works independently of the spin of the concerned resonances: this fact suggests that the parity of the initial state represents really a strong signature in the radiative decay process. To further investigate this effect, the average relative intensities of the strongest low-energy transitions were separately calculated for $J^\pi = 1^+$ and $J^\pi = 1^-$ resonances, respectively. The ratios between these average intensities are plotted in Figs. 24 and 25 for the

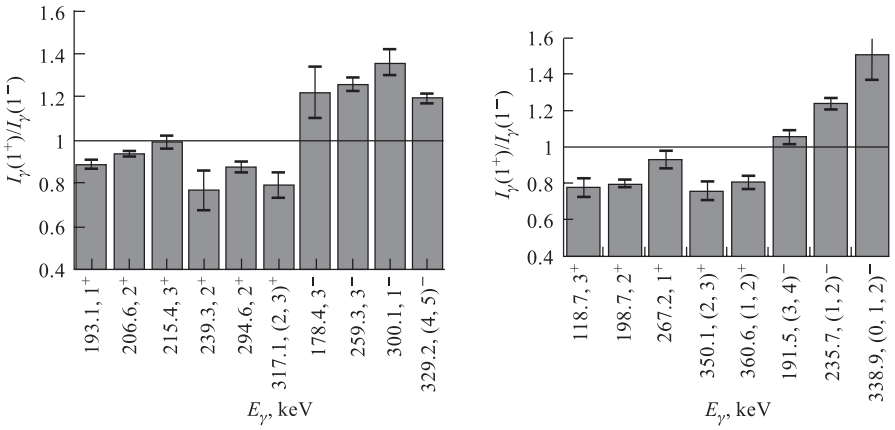

Fig. 24. The parity effect in ^{107}Ag resonances. Each bar represents the ratio between the intensities of the indicated gamma transitions from p resonances with $J^\pi = 1^+$ and s resonances with $J^\pi = 1^-$. These intensities are the averages from several resonances

Fig. 25. Same as Fig. 24 but for ^{109}Ag resonances

relevant low-lying states whose energies and spins and parities are given in abscissa.

It turns out from these data that those low-lying levels of parity opposite to that of the neutron capturing state display a marked tendency to be populated more strongly than the levels with the same parity. The observed effect is on average about $\pm 20\%$. If this effect, established for a limited set of transitions, is due to average statistical properties of the cascade decay of the compound nucleus, it will certainly persist in the cases of all remaining transitions between the low-lying levels. It would also be important to find out whether this parity effect is present only in a few nuclei or whether it is a quite general feature. Unfortunately the data are lacking: for example it is not possible to carry out the same exercise for ^{115}In since no low-energy transition is observed which de-excites negative parity states.

It is important anyway to stress the fundamental difference which exists between the spin dependence of the low-level populations and the parity dependence: the first effect can be explained, at least qualitatively, on very simple grounds and can be reproduced with satisfactory accuracy by the various codes simulating the radiative decay, which have been quoted in the previous sections. On the contrary there is no way of reproducing the parity effect by using the same codes as well as the standard formulae for the γ-ray strength functions and level density as suggested by the various models. In an attempt to understand the observed effect

in terms of photon strength functions, a special experiment devoted to studying two-step cascades following thermal neutron capture in ^{107}Ag, was undertaken at the dedicated facility in Rez. The results of this investigation are published in Ref. 74.

3. SPIN DEPENDENCE OF NUCLEAR QUANTITIES

3.1. Estimates of the Spin Cut-Off Parameter. An obvious and straightforward application of the spin assignment of neutron resonances is the determination of the spin cut-off parameter σ which appears in the level density formula based on the statistical model. The spin-dependent part of this formula, indicated as $\rho(J)$, has already been defined in Eq. (3) of Subsec. 2.1. Its inverse $D(J) = 1/\rho(J)$ is the level spacing. The value of σ can be derived from the ratio $r = D(I - 1/2)/D(I + 1/2)$ according to the formula

$$\sigma \quad = \{(I + 1/2)/\ln[(I + 1)/rI]\}^{1/2}. \tag{4}$$

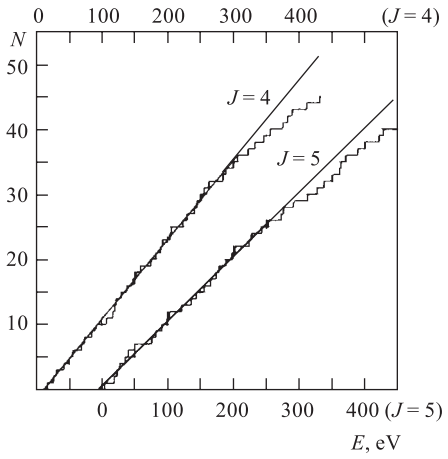

Fig. 26. Cumulative graphs of ^{180}Hf levels assigned to spin $J = 4$ and $J = 5$. The straight lines are obtained from least squares fits in both parameters in the range 0–210 eV

The number of spin assignments needed to determine σ with a given precision depends on the target nucleus spin I and reaches a minimum for $I \cong \sigma$. Since this parameter is estimated to be larger than 3 at the excitation corresponding to the neutron separation energy, it is convenient for this kind of studies to use a target nucleus with rather high spin. For this reason the measurements of ^{177}Hf (with $I = 7/2$) were repeated at CBNM, Geel, and extended to higher energy by using an enriched sample. In addition ^{179}Hf (with $I = 9/2$) was also examined [25, 75]. Another advantage of using these isotopes is that they fall in an atomic mass region with low p-wave strength function so that the probability of observing a resonance with $l = 1$ is negligible. A cumulative graph of the assigned levels is shown in Fig. 26 for the two spin states of ^{180}Hf: a number of 93 resonances were observed up to 430 eV and spin was assigned to 85 of them. However a more accurate determination of σ can be obtained by restricting the analysis to the interval 0–210 eV where apparently

two complete sets of s-wave resonances of known spin are observed as it appears from the good fit with the straight lines in Fig. 26. One can then try to apply to these complete sets the Dyson–Mehta theory which foresees long range correlations between their energy values [1].

Table 5. **Dyson–Mehta statistics for twenty five $J = 4$ and twenty two $J = 5$ resonances of ^{179}Hf (n, γ) with $E < 210$ eV. The values are referred to the CM system**

	$J = 4$ levels		$J = 5$ levels	
	Experiment	DM Model	Experiment	DM Model
Δ_3	0.35	0.32 ± 0.11	0.39	0.31 ± 0.11
Q	8.8	7.9 ± 2.8	6.9	6.9 ± 2.6
$\langle D(J) \rangle$	8.18 ± 0.29 eV		9.64 ± 0.39 eV	

In order to prove that the level positions are more correlated than implied by the Wigner spacing distribution, the «least squares» Δ_3 and the «energy» Q statistics of Dyson and Mehta have been calculated below 210 eV. The agreement between experimental and theoretical values reported in Table 5 is at the same time a proof of the Dyson and Mehta theory and a check of the completeness of the two series. It is then justified to calculate «D(J)» and its standard deviation from the Dyson–Mehta optimum linear statistics. This is very important in order to drastically reduce the uncertainty on «D(J)» with respect to the Wigner distribution of level spacings. In fact Dyson and Mehta [1] have shown that, in the frame of their statistics and for a large number of levels n, the relative standard deviation can be expressed as $\delta D/\langle D \rangle \cong 1/(n-1)$. The resulting estimate of the spin cut-off parameter is then

$$\sigma = 3.70^{+0.32}_{-0.24},$$

where the quoted errors correspond to 68.3% CL.

This accurate result could not be repeated for ^{177}Hf: in this isotope the spin was assigned to 99 out of 105 resonances observed below 300 eV. The cumulative graphs of Fig. 27 show an apparent loss of levels above 180 eV for the $J = 3$ series and above 100 eV for $J = 4$. At 300 eV, the $J = 3$ staircase is 4 levels too low with respect to the straight line while the $J = 4$ staircase is too low by 20 levels. The estimated values

$$\langle 2g\Gamma_n^0 \rangle = 1.1^{+0.6}_{-0.3}\ (\text{meV})^{1/2} \text{ for } J = 3 \text{ and}$$

$$\langle 2g\Gamma_n^0 \rangle = 1.9^{+0.9}_{-0.5}\ (\text{meV})^{1/2} \text{ for } J = 4$$

prevent from concluding that more $J = 4$ than $J = 3$ resonances are missed. Therefore the question arises whether the $J = 4$ level density is actually chang-

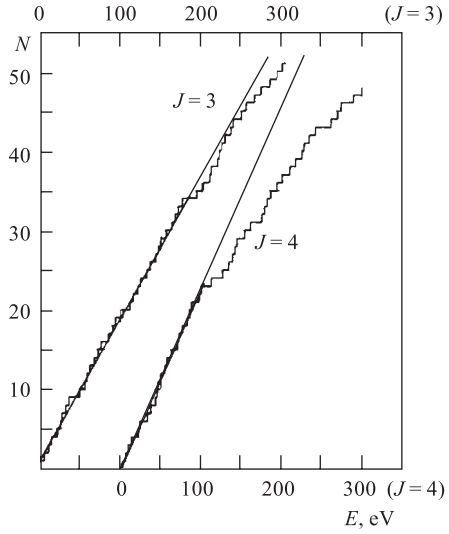

Fig. 27. Cumulative graphs of ^{178}Hf levels assigned to spins $J = 3$ and $J = 4$. The straight lines are obtained from least-squares fits below 180 and 100 eV respectively

ing over the observed energy range. This result suggests that, even at an excitation as high as the neutron separation energy, the level density of the ^{178}Hf compound nucleus may not follow yet the smooth energy dependence foreseen by the statistical model. In this case a σ value determined on such small energy intervals may be unreliable.

Values of the spin cut-off parameter based on the old Dubna data are summarized in Table 6 for a series of target nuclei [76]. One may note that the given errors are much larger than those previously quoted for ^{179}Hf, due to the fact that they have been calculated assuming a Wigner distribution of the level spacings rather than that foreseen by the Dyson–Mehta statistics.

Since in last years more spin assignments have become available for the isotopes of Table 6 as well as for other nuclides, it should be possible to update and extend this table with the aim of obtaining a more accurate and consistent set of values. This exercise requires, for each isotope, a careful selection of the energy interval in which possibly all s-wave resonances are observed and their spins known. The number of levels which are not observed, or vice versa the contamination due to p-wave resonances, should be carefully evaluated and properly taken into account in the estimate of the final errors.

Table 6. **Values of the spin cut-off parameter σ derived from the old Dubna data. The original references are given in the last column**

Nucleus	I	σ	Reference
^{147}Sm	7/2	$7.0^{-2.5}_{+\infty}$	[11]
^{149}Sm	7/2	$12^{-6.5}_{+\infty}$	[11]
^{157}Gd	3/2	$3.5^{-1.0}_{+4.0}$	[13]
^{161}Dy	5/2	$5.0^{-1.7}_{+10}$	[14]
^{163}Dy	5/2	$4.5^{-1.5}_{\infty}$	[14]

3.2. The s-Wave Neutron Strength Function per Spin State. The spin assignment of a large number of neutron resonances with $l = 0$ allows the determination of the s-wave strength function per spin state S_J^0, in a search for a possible spin dependence of such a quantity. The estimate of S_J^0 is less critical than that of the spin cut-off parameter because the failure of observing weak levels affects this quantity in a negligible way.

Values of S_J^0 are listed in Table 7 for a series of twelve target nuclei: also given are the number of resonances per spin state, the investigated energy range and the original references. In the case of relatively recent works, the values of the strengths have been taken directly from the literature while for papers published prior to 1980 the strength functions have been recalculated taking into account both additional spin assignments and the updated values of the neutron widths from the available compilations [77, 78]. The errors, which correspond to the 68.3% CL, have been calculated according to the prescriptions of Liou and Rainwater [79]. One may note that the data are consistent with the assumption of spin independence of the strength function, in agreement with the statistical model, with one exception, namely ^{157}Gd: the probability that in this case the observed differences are accidental is estimated [24] to be less than 3%. However if one uses the older spin assignments of Karzhavina et al. [15] instead of the more recent values of Belyaev et al. [24], the spin difference disappears: in view

Table 7. **Values of the s-wave strength function per spin state for 12 even–odd nuclei**

Target nucleus	I	$S^0_{I-1/2} \cdot 10^4$	$S^0_{I+1/2} \cdot 10^4$	$N^{\rm res}_{I-1/2}$	$N^{\rm res}_{I+1/2}$	$E_{\rm max}$, eV	Reference
^{105}Pd	5/2	$0.99^{+0.39}_{-0.25}$	$0.94^{+0.28}_{-0.20}$	22	32	808	[7]
^{147}Sm	7/2	$4.35^{+1.22}_{-0.78}$	$4.71^{+1.12}_{-0.86}$	40	46	606	[21]
^{149}Sm	7/2	$4.82^{+1.27}_{-0.96}$	$6.17^{+1.48}_{-1.14}$	39	49	255	[13]
^{155}Gd	3/2	$2.08^{+0.74}_{-0.50}$	$1.99^{+0.46}_{-0.36}$	25	49	183	[24]
^{157}Gd	3/2	$1.10^{+0.48}_{-0.30}$	$2.81^{+0.74}_{-0.56}$	19	31	306	[24]
^{161}Dy	5/2	$2.00^{+0.48}_{-0.37}$	$1.93^{+0.42}_{-0.35}$	46	51	312	[15,16]
^{163}Dy	5/2	$2.14^{+0.54}_{-0.41}$	$1.80^{+0.38}_{-0.30}$	43	57	900	[15,16]
^{165}Ho	7/2	1.78 ± 0.20*	1.56 ± 0.14*	27	37	400	[49]
^{167}Er	7/2	$1.88^{+0.56}_{-0.40}$	$2.23^{+0.47}_{-0.38}$	33	58	510	[17]
^{173}Yb	5/2	$1.70^{+0.70}_{-0.45}$	$1.36^{+0.40}_{-0.29}$	20	33	550	[17]
^{177}Hf	7/2	$2.78^{+0.62}_{-0.49}$	$2.09^{+0.49}_{-0.38}$	52	48	303	[25, 51]
^{179}Hf	9/2	$2.21^{+0.85}_{-0.55}$	$2.13^{+0.85}_{-0.55}$	23	21	183	[25, 51]

*Values obtained including also the contribution of the unresolved region up to 2 keV.

of that and in view of the importance of the result, it would be extremely desirable to reinvestigate this isotope and possibly to extend the energy range of the spin determination.

4. SPIN ASSIGNMENT VIA (n, α) REACTIONS

For a number of nuclides the resonance (n, α) reactions occur and can be investigated although their cross sections are extremely small. Nevertheless, this offers an additional possibility to assign the spin to resonance states. Two methods of determination of the resonance spin are available from investigation of those reactions.

The first one is based on the measurement of alpha spectra emitted from individual resonance states of the compound nucleus obtained after s-wave neutron capture with even–odd or odd–even target nuclei of spin I. From the two possible integer values of the spin, $J_1 = I - 1/2$ and $J_2 = I + 1/2$, one is even, and the other is odd.

Let us consider a transition in the alpha decay from the resonance state with spin J_i and parity Π_I to the ground state of a daughter nucleus with spin $J_f = 0$ and parity Π_f. According to the selection rules, the value of the angular momentum «l» may only be carried by the alpha particle emitted in this transition, namely: $l = J_i$. The conservation of the parity decides which of the two possible values of J_i should be chosen, even or odd, according to the relation: $(-1)^l = \Pi_I \cdot \Pi_f$, since the parities of initial states for both the spin values (J_1 and J_2) are the same. The presence of the spectral line corresponding to the considered transition in the alpha spectrum from a resonance state indicates an unambiguous spin value of this state.

This method can be illustrated by the results obtained [81] for the even–odd target nucleus ^{147}Sm. The possible spin values of the s-wave resonance states of ^{147}Sm are $J_i = 3$ and 4, and their parity is $\Pi_I = -1$. The ground state of the daughter even–even nucleus ^{144}Nd has $J_f = 0$ and $\Pi_f = +1$. Therefore, according to the above-mentioned relation, solely the odd value $l = J_1 = 3$ is allowed while the other one is forbidden. Thus, the spin value 3 should be assigned to the resonances whose alpha spectra exhibit the transition to the ground state of the daughter nucleus.

The alpha spectra for 11 resonances of the ^{147}Sm target are shown in Fig. 28. The presence of the spectral line corresponding to the considered transition is undoubtedly observed for the resonances: 3.4, 29.7, 83.3, 123.4, and 183.7 eV to which spin $J_1 = 3$ is assigned.

The lack or doubtful occurrence of the considered line in the experimental alpha spectra from some resonance states (as for resonances 32.1 (Fig. 28, a) and 57.9 eV (Fig. 28, k)) cannot be interpreted as a credible evidence of resonance

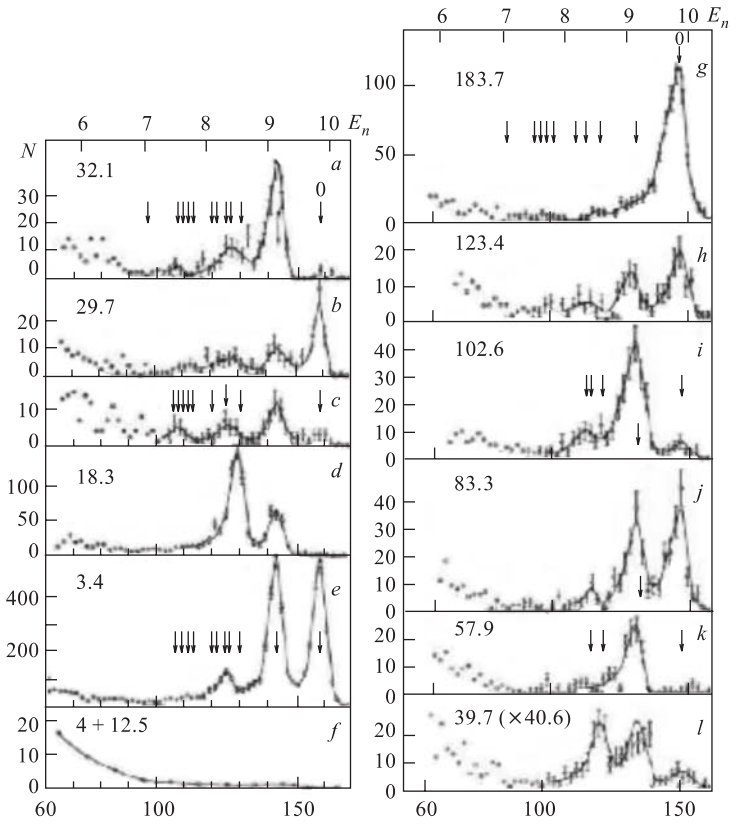

Fig. 28. The alpha spectra from ^{147}Sm resonances. The energies of the resonances in eV are indicated over the spectra. The spectral line corresponding to the transition to the ground state of the daughter nucleus is indicated by an arrow marked «0»

spin $J_2 = 4$. This is because the partial alpha widths for this transition (if it is allowed) fluctuate according to the Porter–Thomas distribution. Consequently, one cannot exclude that a given width falls below the observability threshold of the detection system for the relevant resonance.

The measurement of alpha spectra from the resonance reaction is rather a difficult task because of its extremely small cross section and the necessity to use very thin targets to avoid worsening of the energy resolution of the alpha lines. The investigation of total cross sections of the (n, α) reaction is not subject to the same restriction as in the measurement of the alpha spectra. The second

method of the resonance spin determination from the (n, α) reaction is based on the comparison of the average values and distributions of total alpha widths corresponding to each resonance spin value. The theoretical basis of the method has been presented in Ref. 82, and tested with the ^{143}Nd [82] and ^{147}Sm [81] target nuclei. A short outline of the theoretical foundation of the method is given below.

The partial alpha width of the resonance λ for the transition to a daughter nucleus state «f» of an alpha particle with angular momentum «l» is usually written as:

$$\Gamma_{\lambda c} = 2\gamma_{\lambda c}^2 P_c, \tag{5}$$

where c (f, l) stands for the characteristics of the decay exit channel; P_c is the barrier penetration for the alpha particle, and $2(\gamma_{\lambda c})^2$ is the reduced partial alpha width. The total alpha width of a resonance λ is the sum of all partial alpha widths of the transitions allowed by the selection rules

$$\Gamma_\lambda = \sum_c \Gamma_{\lambda c} = 2 \sum_c \gamma_{\lambda c}^2 P_c. \tag{6}$$

Following the idea of the statistical model of the compound nucleus [83] we assume that the reduced partial alpha widths obey the Porter–Thomas distribution, and that the average value of these widths is independent of the exit channel «c» and the resonance spin J_i, where «I» is 1 or 2. Then the average total alpha width for resonances with a given spin J is

$$\langle \Gamma_\lambda \rangle_J = \sum_c \langle \Gamma_{\lambda c} \rangle_J = 2 \langle \gamma_{\lambda c}^2 \rangle_J \sum_c P_{cJ}. \tag{7}$$

The dependence of the $\langle \Gamma_\lambda \rangle_J$ on the resonance spin comes from different sets of P_c allowed by selection rules for resonances with different spins.

As it has been shown in Ref. 82, the accepted assumption allows one to describe approximately the distributions of the total alpha widths for the resonances with spin J by the chi-squared function with the number of degrees of freedom

$$\nu_J = \frac{\left(\sum\limits_c P_{cJ} \right)^2}{\sum\limits_c P_{cJ}^2} \tag{8}$$

and by the average value (7).

Since the sets of the barrier penetration for both resonance spins are different, the distributions of the total alpha widths belonging to resonances with different spins have different values of both ν_J and $\langle \Gamma_\lambda \rangle_J$. Thus the theoretical distributions of the total alpha widths corresponding to resonances with different

spins are different, and their total distribution is the weighted superposition of the particular distributions.

To compare the experimental distribution of the total alpha widths of resonances which have unknown spins with the theoretical predictions, one should find the average values of $\langle\Gamma_\lambda\rangle_1$ and $\langle\Gamma_\lambda\rangle_2$ for the separate spin groups and normalize them to the experimental average over both spin values $\langle\Gamma_\lambda\rangle_{\rm exp}$. For this purpose one can use two relations

$$\rho_1\langle\Gamma_\lambda\rangle_1 + \rho_2\langle\Gamma_\lambda\rangle_2 = \rho\langle\Gamma_\lambda\rangle_{\rm exp}, \tag{9}$$

$$\frac{\rho_1\langle\Gamma_\lambda\rangle_1}{\rho_2\langle\Gamma_\lambda\rangle_2} = \frac{\left(\sum\limits_c P_c\right)_1}{\left(\sum\limits_c P_c\right)_2}, \tag{10}$$

where

$$\rho(J) = \rho_0(2J+1)\,\exp\left[-\frac{(J+1/2)^2}{2\sigma^2}\right] \tag{11}$$

and

$$\rho = \rho_1 + \rho_2 = \rho(J_1) + \rho(J_2).$$

The values of P_c are tabulated [84] or can be calculated. From the found values of $\langle\Gamma_\lambda\rangle_J$ and ν_J the individual distribution can be obtained as the chi-squared form

$$p_J(x,\nu_J,\langle x\rangle_J) = \frac{(n)^n}{\Gamma(n)\langle x\rangle_J^n}x^{n-1}\,\exp\left(-n\frac{x}{\langle x\rangle_J}\right), \tag{12}$$

where $n = \nu_J/2$, x stand for the Γ_λ, and $\Gamma(n)$ is the gamma function.

To compare this theoretical distribution with the experimental one for rather small numbers «r» of resonances of unknown spins (for both resonance spin groups), it is more convenient to calculate the integral distribution normalized to the number «r» of investigated resonances.

This distribution is

$$rP(\Gamma_\lambda > x) = \frac{r}{\rho}\left(\rho_1\int\limits_x^\infty p_1(x)\,dx + \rho_2\int\limits_x^\infty p_2(x)\,dx\right). \tag{13}$$

Function (13) superimposed on the experimental histogram $N(\Gamma_\lambda > \Gamma)$ is represented by a full line in Fig. 29 for the total widths of the ^{147}Sm target nucleus [81]. In the upper part of Fig. 29 the probability to find a width belonging to a resonance with $J_1 = 3$ is shown. That probability is given by the relation:

$$\eta(J_1) = \frac{r_1p_1(x)}{r_1p_1(x)+r_2p_2(x)} = \frac{\rho_1p_1(x)}{\rho_2p_2(x)}\left(1+\frac{\rho_1p_1(x)}{\rho_2p_2(x)}\right)^{-1}. \tag{14}$$

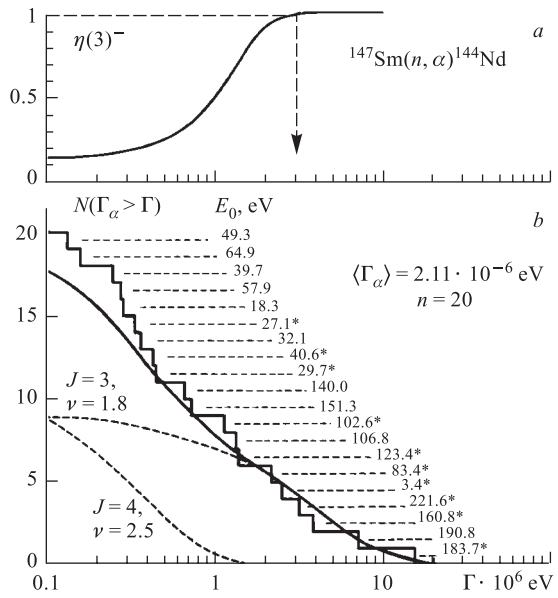

Fig. 29. *a*) The probability that a resonance with a given alpha width has spin $J = 3$. The vertical dashed line marks the alpha width corresponding to 0.99 probability. *b*) The integral distribution of total alpha widths for both spin resonances of ^{147}Sm obtained from experiment (histogram) compared to the expected theoretical distributions for individual spin states (dashed lines) and to their sum (solid line). Asterisks at resonance energies denote those $J = 3$ resonances whose spin was assigned by observation of the ground state transition

A distribution similar to that of Fig. 29 has been presented in Ref. 82 for the ^{143}Nd target nucleus.

The reliability of this method of determination of the neutron resonance spin strongly depends on the difference between the ΣP_c values of both resonance spin states. For even–even compound nuclei this increases considerably with the energy of the first excited level of the daughter nucleus. That causes the strong variation from unity of the ratio $\langle\Gamma_\lambda\rangle_1/\langle\Gamma_\lambda\rangle_2$ which determines the relative shift of the distributions of the total alpha widths belonging to different resonance spins and makes spin separation possible [82].

CONCLUSIONS

An inspection of the compilations of neutron resonance parameters [77, 78] shows that, besides isotopes for which the knowledge of resonance spins is satis-

factory, there are others for which the column of J values presents many voids particularly on the high energy side. The message of the present review is that most of these voids can be filled by using the techniques described in the previous chapters.

These tecniques apply to those nuclei for which radiative capture follows the statistical model, namely most nuclei with $A > 90$–100, with the exception of magic or near-magic nuclides. The multiplicity method has the merit of having provided large amounts of spin assignments at times (end of sixties, beginning of seventies) which were technologically less advanced on any experimental aspect: neutron sources, detectors, data acquisition systems. However, the main limit of this technique is the fact of not being applicable to odd–even target nuclei. The low-lying level population method is not subject to this limitation while presenting at the same time spin effects much larger than those of the multiplicity method. The success in determining the spin of several weak p-wave resonances is the best proof that the method is powerful enough to be applied even in extreme experimental situations. The extension of the population method to the parity assignment of neutron resonances is a recent exciting development still awaiting an experimental explanation. Finally, spin assignment via (n, α) reactions is an interesting technique which has however limited application in view of the smallness of the cross sections and the need to use very thin samples.

Acknowledgements. First of all the authors wish to express their heartiest gratitude to Yuri Popov for having suggested the writing of the present review. In addition one of them (F. C.) is very grateful to Albert Popov for having provided a complete summary in English of the activity performed in Dubna in relation with the multiplicity method. They are also indebted to Frank Gunsing, Luca Zanini, Peter Siegler and Judy Kennedy for having prepared most of the figures. Finally, they would like to thank Claudio Coceva for a critical reading of the manuscript and useful suggestions.

REFERENCES

1. *Dyson F. J., Mehta M. L.* // J. Math. Phys. 1963. V. 4. P. 701.
2. *Allen B. J.* Neutron Radiative Capture / Ed. by R. Chrien. Oxford, 1984. P. 1.
3. *Lone M. A. et al.* // Phys. Rev. 1968. V. 174. P. 1512.
4. *Coceva C.* // Nuovo Cim. 1994. V. 107. P. 85.
5. *Bollinger L. M., Coté R. E., Jackson H. E.* // Compt. Rend. Cong. Intern. de Physique Nucléaire, Paris, July 2–8, 1964. V. 2. P. 673.
6. *Coceva C. et al.* // Proc. of the Intern. Conf. on Neutron Cross Sections and Technology, Washington, 1968. V. 2. P. 897.
7. *Coceva C. et al.* // Nucl. Phys. A. 1968. V. 117. P. 586.
8. *Draper J. E., Springer T. E.* // Nucl. Phys. 1960. V. 16. P. 27.

9. *Ericson T.* // Adv. Phys. 1960. V. 9. P. 425.
10. *Giacobbe P., Stefanon M., Dellacasa G.* CNEN Techn. Report RT/FI (68) 20. 1968.
11. *von Egidy T.* // Proc. of the Intern. Symp. on Neutron Capture Gamma Ray Spectroscopy, Studsvik, 1969. Vienna, 1969. P. 541.
12. *Karzhavina E. N., Kim Sek Su, Popov A. B.* JINR Preprint P3-6092. Dubna, 1971.
13. *Karzhavina E. N., Kim Sek Su, Popov A. B.* JINR Preprint P3-6237. Dubna, 1972.
14. *Karzhavina E. N., Kim Sek Su, Popov A. B.* // Proc. of the Intern. Conf. on Nuclear Studies with Neutrons, Budapest, 1972. Contrib. P. 20.
15. *Karzhavina E. N., Kim Sek Su, Popov A. B.* JINR Preprint P3-6948. Dubna, 1973.
16. *Karzhavina E. N. et al.* // Yad. Fiz. 1975. V. 22. P. 3.
17. *Karzhavina E. N. et al.* JINR Preprint P3-8511. Dubna, 1975.
18. *Muradyan G. V. et al.* // Proc. of the Intern. Conf. on Neutron Cross Sections for Technology, Knoxville, USA, 1979. P. 521.
19. *Danilin B. V. et al.* // Atom. Ener. 1985. V. 58. P. 178.
20. *Janeva N. et al.* // Nucl. Instr. Meth. 1992. V. 313. P. 266.
21. *Georgiev G. et al.* // Nucl. Phys. A. 1993. V. 565. P. 643.
22. *Georgiev G. et al.* // Bulg. J. Phys. 1991. V. 18. P. 1.
23. *Efimov B. V. et al.* // Proc. of the 1st Intern. Conf. on Neutron Physics, Kiev, 1987. V. 2. P. 214.
24. *Belyaev F. N. et al.* // Yad. Fiz. 1990. V. 52. P. 625.
25. *Coceva C. et al.* CNEN Techn. Report RT/FI (70) 55. 1970.
26. *Coceva C.* Private communication.
27. *Pönitz W. P.* // Z. Physik. 1966. V. 197. V. 262.
28. *Huizenga J. R., Vandenbosch R.* // Phys. Rev. 1960. V. 120. P. 1305.
29. *Domanic F., Sailor V. L.* // Ibid. V. 119. P. 208.
30. *Stolovy A.* // Ibid. V. 118. P. 211.
31. *Fenstermacher C. A., Draper J. E., Bockelman C. K.* // Nucl. Phys. 1959. V. 10. P. 386.
32. *Vonach H. K., Vandenbosch R., Huizenga J. R.* // Nucl. Phys. 1964. V. 60. P. 70.
33. *Troubetzkoy E. S.* // Phys. Rev. 1961. V. 122. P. 212.
34. *Sperber D.* // Nucl. Phys. A. 1967. V. 90. P. 665.
35. *Sperber D., Mandler J. W.* // Nucl. Phys. A. 1968. V. 113. P. 689.
36. *Weisskopf V. W.* // Phys. Rev. 1951. V. 83. P. 1073.
37. *Moskowski S. A.* // Phys. Rev. 1953. V. 89. P. 474.
38. *Wetzel K. J., Thomas G. E.* // Phys. Rev. C. 1970. V. 1. P. 1501.
39. *Pönitz W. P.* // Bull. Am. Phys. Soc. 1968. V. 13. P. 1389.
40. *Pönitz W. P., Tatarczuk J. R.* // Nucl. Phys. A. 1970. V. 151. P. 569.
41. *Bhat M. R. et al.* // Phys. Rev. C. 1970. V. 2. P. 1115.
42. *Bhat M. R. et al.* // Ibid. P. 2030.
43. *Stolovy A. et al.* // Phys. Rev. 1967. V. 155. P. 1330.

44. *Asghar M., Moxon M. C., Chaffey C. M.* // Proc. of the Intern. Conf. on the Study of Nuclear Structure with Neutrons, Antwerp, 1965. North Holland Publ. Comp., 1966.
45. *Stolovy A. et al.* // Phys. Rev. C. 1972. V. 5. P. 2030.
46. *Corvi F. et al.* // Nucl. Phys. A. 1973. V. 203. P. 145.
47. *Keyworth G. A. et al.* // Phys. Rev. Lett. 1973. V. 31. P. 1077.
48. *Corvi F., Stefanon M.* // Nucl. Phys. A. 1974. V. 223. P. 185.
49. *Coceva C., Giacobbe P.* // Nucl. Phys. A. 1977. V. 293. P. 167.
50. *Aldea L. et al.* // Czech J. Phys. B. 1978. V. 28. P. 17.
51. *Olejniczak U. et al.* // Yad. Fiz. 2002. V. 65. P. 2105.
52. *Coceva C. et al.* // Nucl. Phys. A. 1974. V. 218. P. 61.
53. *Breitig D. et al.* // Phys. Rev. C. 1974. V. 9. P. 366.
54. *Sushkov O. P., Flambaum V. V.* // Sov. Phys. Usp. 1982. V. 25. P. 1.
55. *Bunakov V. E., Gudkov V. P.* // Nucl. Phys. A. 1983. V. 401. P. 93.
56. *Alfimenkov V. P. et al.* // Ibid. V. 398. P. 93.
57. *Zhu X. et al.* // Phys. Rev. C. 1992. V. 46. P. 768.
58. *Frankle C. M. et al.* // Ibid. P. 778.
59. *Crawford B. E. et al.* // Phys. Rev. C. 1998. V. 58. P. 1225.
60. *Stephenson S. L. et al.* // Ibid. P. 1236.
61. *Seestrom S. J. et al.* // Ibid. P. 2997.
62. *Lowie L. Y. et al.* // Phys. Rev. C. 1999. V. 59. P. 1119.
63. *Crawford B. E. et al.* // Ibid. V. 60. P. 055503.
64. *Stephenson S. L. et al.* // Phys. Rev. C. 2000. V. 61. P. 045501.
65. *Corvi F. et al.* // Proc. of the Intern. Conf. on Nuclear Data for Science and Technology, Gatlinburg, Tennessee, USA, May 9–13, 1994. P. 201.
66. *Gunsing F. et al.* // Phys. Rev. C. 1997. V. 56. P. 1266.
67. *Zanini L.* Ph. D. Thesis. Delft University of Technology, 1998.
68. *Zanini L. et al.* // Phys. Rev. C. 2000. V. 61. P. 054616-1.
69. *Postma H.* // Proc. of the 2nd Intern. Seminar on Interaction of Neutrons with Nuclei, Dubna, April 26–28, 1994.
70. *Becvar F., Ulbig S.* DICEBOX Computer Code. Prague: Charles University, 1991.
71. *Gunsing F.* // Nucl. Instr. Meth. A. 1995. V. 365. P. 410.
72. *Eadie W. T. et al.* Statistical Methods in Experimental Physics. Amsterdam: North Holland, 1971.
73. *Bollinger L. M., Thomas G. E.* // Phys. Rev. 1968. V. 171. P. 1293.
74. *Zanini L. et al.* // Phys. Rev. C. 2003. V. 68. P. 014320.
75. *Coceva C. et al.* Statistical Properties of Nuclei / Ed. by J. B. Garg. N. Y., 1972. P. 447.
76. *Popov A. B.* Private communication.
77. *Mughabghab S. F., Divadeenam M., Holden N. E.* Neutron Cross Sections. N. Y.: Academic Press, 1981.

78. *Sukhoruchkin S. I., Soroko Z. N., Deriglazov V. V.* // Low Energy Neutron Physics / Ed. by H. Schopper, L. Boernstein. Darmstadt, 1998. V. 16B.

79. *Liou H. E., Rainwater J.* // Phys. Rev. C. 1972. V. 6. P. 435.

80. *Coceva C.* Private communication.

81. *Popov Yu. P. et al.* // Nucl. Phys. A. 1972. V. 188. P. 212.

82. *Popov Yu. P. et al.* // Acta Phys. Polon. B. 1973. V. 4. P. 275.

83. *Porter C. E., Thomas R. C.* // Phys. Rev. 1956. V. 104. P. 483.

84. *Dadakina A. F.* // Bull. Inform. Centre on Nucl. Data. M., 1968. P. 226.